Study on efficient and accurate protocols of measuring sorption isotherm of porous building materials using three-dimensional hygrothermal simulation

Fukui, Kazuma

Takada, Satoru

Title

Study on efficient and accurate protocols of measuring sorption isotherm of porous building materials using three-dimensional hygrothermal simulation

Authors

Kazuma Fukui[1,*], Satoru Takada[1]

[1]Kobe university, Graduate School of Engineering, 1-1, Rokkodai-cho, Nada-ku, Kobe 657-8501, Japan

*Coresponding author
Email Address: fukui@peridot.kobe-u.ac.jp
Phone No: +81-78-803-6060

1 Introduction

Moisture transfer in porous building materials affects the energy consumption of buildings (Woloszyn, et al., 2009; Martínez-Marino, et al., 2021; Wan, et al., 2021), durability of the materials (Nakajima, et al., 2020; Sakiyama, et al., 2021; Parracha, et al., 2021), and comfort and health of the occupants (Woloszyn, et al., 2009; Martínez-Marino, et al., 2021). Thus, hygrothermal models have been developed and are widely used to predict heat and moisture transfer in building components (Woloszyn, et al., 2009; Sakiyama, et al., 2021; Delgado, et al., 2010; Shi, et al., 2018; Asphaug, et al., 2021). Numerical calculations using these models require the hygric properties of materials, such as sorption/desorption curves, suction curves, moisture diffusion resistance factors (or moisture permeability), and liquid conductivity. Fortunately, databases of the properties of common building materials are available (Kumaran, 1996, 2006) and are often provided in simulation software (WUFI, Fraunhofer IBP; DELPHIN, Bauklimatik Dresden). However, even in recent years, considerable effort has been expended, out of necessity, in measuring the hygric properties of materials to examine the relationships between material properties and composition (McGregor, et al., 2014; Ma, et al., 2020; Yang, et al., 2021), environmental and experimental conditions (Fabbri, et al., 2017; Fabbri and McGregor, 2017; Promis, et al., 2019; Zhang and Richman, 2021), types and concentrations of absorbed solutions (Luan, et al., 2020), age (Zhang and Richman, 2020, 2021), hysteresis effects (Zhang, et al., 2016), or damage states (Zhang, et al., 2017; Wang, et al., 2019; Bao, et al., 2020). In addition, it is important to measure the properties of natural materials, such as stone (Yamada, et al., 2020; Banfill, 2021) and materials used in historic buildings (Zhao, et al., 2019), whose properties vary widely depending on the production area and period.

The sorption property of a material in the hygroscopic region (sorption isotherm) is one of the most important hygric properties for hygrothermal simulations (EN 15026). This property relates humidity to the moisture content and is commonly used in the form of moisture capacity in moisture mass balance equations. The sorption properties are important for evaluating the moisture buffering effects of materials. In addition, they affect the heat and moisture transfer in materials because these are functions of the moisture content. The static desiccator method using saturated salt solution is a more common and simpler method of obtaining sorption isotherms compared to other methods such as dynamic methods (Tada and Watanabe, 2005; Rode and Hansen, 2011; Chen and Chen, 2014; Bui, et al., 2017); it is standardized by many international and national standards, such as ISO 12571, ASTM C1498, and JIS A 1475.

ISO 12571 specifies that the mass of a specimen should be periodically measured until in equilibrium with the environment, where equilibrium is determined to exist if the change in mass between three consecutive weightings, each made at least 24 h apart, differs by less than 0.1%. Thus, the frequency and time for conducting mass measurements to confirm equilibrium is decided by those who conduct the measurements, which can take considerable time and effort; frequent mass

measurements are effort-consuming and even prolong the sorption/desorption processes owing to disturbance from the environment or the mass measurement procedure itself. Conversely, a long measurement interval may result in loss of time and energy when sorption or desorption is faster than expected. In addition, prolonged measurement causes risks of inaccurate results owing to mold and mildew growth. Moreover, the mass of the specimens often continues to change at a rate of <0.1% per day, resulting in a non-negligible difference in the calculated moisture content. Therefore, there are considerable risks of underestimation of the equilibrium moisture content if the attainment of equilibrium is judged as specified in ISO 12571.

Because it takes time before a specimen reaches equilibrium with air in a desiccator, the measurement process can extend for several weeks or even months (Feng, et al., 2013); thus, several studies to enhance the efficiency of the desiccator method have been conducted (Feng, et al., 2013; Peuhkuri, et al., 2005). However, to attain more efficient measurements without losing accuracy, the optimum measurement protocol for materials with various hygric properties should be investigated from the perspective of judging the attainment of the equilibrium.

Therefore, in this study, we examined possible improvements and error risks in determining the attainment of equilibrium for a static desiccator method based on the adsorption processes of typical building materials. We developed a calculation model for three-dimensional simultaneous heat and moisture transfer in a material corresponding to the measurement procedure specified in ISO 12571 and simulated the changes in the distribution of temperature and moisture content in the sorption isotherm measurement process; the evolution of the amount of adsorbed moisture in a specimen and time to reach equilibrium during measurement were calculated for five different materials whose properties are provided in an international database. The calculated results were compared with the measurement results for one material (autoclaved aerated concrete (AAC)). Thereafter, numerical simulations were conducted to examine the effects of the hygric properties of a material, humidity level, and specimen dimensions. Based on the results, we discussed suitable measurement times and frequencies and possible errors for each type of material and various experimental conditions.

2 Three-dimensional hygrothermal model

2.1 Fundamental equations

We employed the same equations as those used in the WUFI ® software (Fraunhofer IBP) to reproduce the sorption processes during measurement using the desiccator method. The fundamental equations used in the calculation were derived from the heat and moisture mass conservation equations wherein the moisture transfer is based on Fick's law of diffusion (Künzel, 1995):

$$\frac{\partial H}{\partial \theta}\frac{\partial \theta}{\partial t} = \nabla \cdot (\lambda \nabla \theta) + h_v \nabla \cdot \left(\frac{\delta}{\mu} \nabla p \right) \tag{1}$$

$$\rho_w \frac{\partial u}{\partial \varphi}\frac{\partial \varphi}{\partial t} = \nabla \cdot \left(\rho_w D_w \frac{\partial u}{\partial \varphi} \nabla \varphi \right) + \nabla \cdot \left(\frac{\delta}{\mu} \nabla p \right), \quad (2)$$

where D_w is the moisture diffusivity (m²/s), h_v is the evaporation enthalpy of water (2.44×10^6 J/kg), p is the water vapor partial pressure (Pa), u is the moisture content (m^3/m^3), δ is the water vapor diffusion coefficient in air (kg/(m·s·Pa)), θ is the temperature (°C), λ is the heat conductivity of moist material (W/(m·K)), μ is the vapor diffusion resistance factor of dry material, ρ_w is the density of liquid water (kg/m^3), and φ is the relative humidity. H is the sum of the enthalpies of moisture and dry building materials (Künzel, 1995):

$$H = (\rho_s c_s + u \rho_w c_w)\theta, \quad (3)$$

where c_s and c_w are the specific heats (J/(kg·K)) of a material and liquid water, respectively, and ρ_s is the density of the dry bulk material (kg/m^3). The factor of proportionality relating the vapor pressure gradient in Equation (2) (i.e., δ / μ) is the vapor permeability of the material (kg/(m·s·Pa)).

2.2 Materials

To compare the rates of adsorption of materials with different hygric properties, we selected five types of materials with broad ranges of properties; concrete, AAC and gypsum board (GB), and pine and oriented strand board (OSB) were chosen as examples of cement-based materials, board materials, and wooden materials, respectively. The material properties were derived from the databases of the International Energy Agency (IEA) Annex 24 project (Kumaran, 1996) and ASHRAE Research Project 1018-RP (ASHRAE, 2002). Table 1 lists the densities, specific heats, and vapor permeabilities of the materials.

Table 1. Densities, specific heats, and vapor permeabilities of the materials used in the calculation

		Density	Specific heat	Vapor permeability	Source
		kg/m^3	J/(kg·K)	kg/(m·s·Pa)	
Concrete		2200	840	1.26×10^{-12}	Kumaran 1996
Autoclaved aerated concrete		500	840	1.80×10^{-11}	
Gypsum board		700	870	3.30×10^{-11}	
Pine	Transversal direction	400	1880	2.60×10^{-13}	
	Longitudinal direction			2.90×10^{-11}	
Oriented strand board		650	1880	Function of humidity	ASHRAE 2002

Figure 1 shows the sorption isotherms of the materials. We used the sorption curve functions provided by Kumaran (1996) for pine while constructing curves that fit the provided discrete values for concrete, AAC, GB, and OSB. The dependence of the thermal conductivity on the moisture content was considered for concrete and AAC, as shown in Fig. 2. The thermal conductivity of wet material is not provided in the database for GB, pine, or OSB, and the dependency on the moisture content was not considered in the simulation. The thermal conductivities of GB and OSB are 0.24 and 0.10 W/m·K, and that of pine is 0.25 and 0.1 W/m·K in the longitudinal and transverse directions, respectively. Finally, the moisture diffusivity of the materials as a function of relative humidity is shown in Fig. 3 (a). As few data are available for the dependency of the moisture diffusivity of the OSB on humidity, the changes in its moisture transfer properties are considered as the dependency of the vapor permeability on humidity, as shown in Fig. 3 (b). We used the same transport properties for all directions for the OSB, although it has anisotropic properties owing to the orientation of wood strands. This was because of the lack of readily available data in the literature for the properties in different orientations.

[insert Figure 1]
[insert Figure 2]
[insert Figure 3]

2.3 Calculation models and conditions

Currently, WUFI can consider one- and two-dimensional heat and moisture transport in building materials. Here, for the measurement simulations, we developed a computer program for three-dimensional transport. We developed a calculation model assuming that the specimen was cubic, as shown in Fig. 4. The origin of the rectangular coordinate system was set at the center of the model. For pine, which had anisotropic properties, the properties in the longitudinal and transverse directions were applied in one (x-axis) and two (y- and z-axes) directions, respectively. The calculation was conducted in one-eighth of the model, considering that the specimens were symmetric.

[insert Figure 4]

Feng et al. (2013) showed that small specimens can reduce the time required to reach equilibrium without sacrificing accuracy. To demonstrate the effects of the specimen size on the rate of adsorption, we considered four model sizes, as shown in Table 2. For the first two cases (Cases A and B), the volume of the specimen(s) was set to approximately 10 000 mm^3. It was assumed that the specimen was divided into three pieces to reduce the time to reach equilibrium for Case A; the edge length of the specimens was set to 15 mm (10 125 mm^3 in volume). For Case B, one specimen had a 10 000

mm^3 volume, and the edge lengths were set to 22.2 mm. For Case C, it was assumed that one specimen had a mass of 10 g, which is the lower limit of the specimen mass provided in ISO 12571. The edge length of the specimen differed depending on the density of the material and was set to 16.2 mm, 27.0 mm, 24.6 mm, 29.4 mm, and 24.6 mm for concrete, AAC, GB, pine, and OSB, respectively. For concrete, these sizes were smaller than those used for the general tests, and an additional calculation case (Case D) was added wherein the edge length of a cubic specimen was set to 100 mm.

The basic equations were discretized using the finite difference method. The forward and central differences were used for time and space, respectively. The time and space steps were set to 0.04 s and 0.6 mm, respectively.

The initial temperature and relative humidity of the material were set to 23.0 °C and 0%, respectively, assuming that the measurement was conducted during the sorption processes. The Robin boundary condition was used for both the temperature and humidity, and the heat and moisture fluxes on the surfaces were calculated from Equations (4) and (5), respectively:

$$q = (\alpha_c + \alpha_r)(\theta_a - \theta_s) \tag{4}$$

$$g_v = \beta_p (p_a - p_s), \tag{5}$$

where g_v is the water vapor flux density (kg/(m^2·s)); q is the heat flux density (W/m^2); α_c and α_r are the convective and radiative heat transfer coefficients (W/(m^2·K)), respectively; and β_p is the water vapor transfer coefficient (kg/(m^2·s·Pa)). Subscripts a and s represent the ambient air and material surface, respectively. The temperature of the surrounding air was set to 23.0 °C. The relative humidity was set to 33%, 53%, 75%, and 93%, as provided in ISO 12571, which could be achieved using magnesium chloride ($MgCl_2 \cdot 6H_2O$), magnesium nitrate ($Mg(NO_3)_2 \cdot 6H_2O$), sodium chloride (NaCl), and potassium nitrate (KNO_3), respectively, at 23.0 °C. The calculation conditions, including the target humidity, are summarized in Table 3. We hereinafter refer to each calculation case using an abbreviation. For example, calculation "C-33-A" represents a calculation in which the material properties of concrete are used, the target humidity is set to 33%, and case A is used for the specimen dimensions.

Table 2. List of cases of specimen dimensions for the numerical simulations

Case A	Three cubic specimens with 15 mm edges
Case B	One cubic specimen with 22.2 mm edges
Case C	One cubic specimen with 10 g mass (lower limit of the specimen mass provided in ISO 12571)
Case D (only for concrete)	One cubic specimen with 100 mm edges

Table 3. Calculation conditions

Calculation Cases	Material	Target humidity	Specimen dimensions*			
			A (15 mm edges)	B (22.2 mm edges)	C (10 g mass)	D (100 mm edges)
C-33-	Concrete	33%	✓**	✓	✓	✓
C-53-		53%				
C-75-		75%				
C-93-		93%				
AAC-33-	Autoclaved aerated concrete (AAC)	33%	✓	✓	✓	Not calculated
AAC-53-		53%				
AAC-75-		75%				
AAC-93-		93%				
GB-33-	Gypsum board (GB)	33%	✓	✓	✓	Not calculated
GB -53-		53%				
GB -75-		75%				
GB -93-		93%				
P-33-	Pine	33%	✓	✓	✓	Not calculated
P-53-		53%				
P-75-		75%				
P-93-		93%				
OSB-33-	Oriented strand board (OSB)	33%	✓	✓	✓	Not calculated
OSB-53-		53%				
OSB-75-		75%				
OSB-93-		93%				

* Cases for specimen dimensions are shown in Table 2.

**Check marks indicate tested conditions.

Considering that the air velocity in a desiccator is remarkably low, the convective heat transfer and moisture transfer on the surface of a material were expected to be small. The moisture transfer coefficient between the air and material surfaces was set to 4.86×10^{-9} kg/(m^2·s·Pa) and the convective heat transfer coefficient was calculated to 0.8 W/(m·K) using the Lewis relationship (Eckert & Drake, 1987) with a Lewis number of 1.0. The radiative heat transfer coefficient was set to 4.7 W/(m·K).

3 Comparison of simulated and measured results

3.1 Measurements for comparison

To obtain the measurements for the comparison, we used an AAC board manufactured by Sumitomo Metal Mining Siporex Co., Ltd. The material age was more than four years. Cubic specimens with approximately 15 mm edges were sliced from the board, and three specimens were used for the measurements (corresponding to calculation Case A). The specimens are shown in Fig. 5 (a). The specimens were oven-dried for approximately 6 days at 105 °C before measurement. It was confirmed that the mass of the specimens reached a steady value (fluctuating at 0.1%).

[insert Figure 5]

It is necessary to open the lid of a desiccator during the general desiccator method to weigh the specimens, which may cause fluctuations in the humidity in the desiccator and affect the sorption/desorption processes. To minimize such disturbances from the environment and obtain suitable data for comparison, we conducted measurements using a glass jar referring to ISO 12571 Annex D. The experimental setup is illustrated in Fig. 5 (b). The height and diameter of the jar were 135 mm and 98 mm, respectively. The jar had a metal dish inside, which was suspended by a thin metal wire to hold the specimens in humidity-controlled air. The lid of the jar had a tiny hole, which allowed the mass measurement of the specimens by means of suspended weighting. The hole was covered by aluminum foil and tape except during the mass measurement. An electronic scale with sufficient readability (0.1 mg) and repeatability (0.05 mg) was employed.

To control the humidity in the jar, we used a saturated salt solution of NaCl, which controlled the relative humidity of the surrounding air at 75.36 ± 0.13% at 23.0 °C. The jar was placed in a climatic chamber in which the temperature was maintained at 23.0 ± 0.5 °C.

3.2 Comparison of the measured and calculated results

Figure 6 compares the measurement results with the calculated results. The calculations were performed under the AAC-75-A conditions described in Table 3 in accordance with the experiment. To check the adequacy of the moisture transfer coefficient at the surfaces of the specimens used in the calculations, the calculated results with three different values of 2.43×10^{-9}, 4.86×10^{-9}, and 9.72×10^{-9} kg/(m^2·s·Pa) are shown. Rapid adsorption in the initial stage of the measurement (several hours after the beginning of the adsorption) was well reproduced when the moisture transfer coefficient was set to 4.86×10^{-9} kg/(m^2·s·Pa), although the calculated results for the amount of the adsorbed moisture during the next few days were slightly larger than the measured results, as shown in Fig. 6. The root-mean-square errors between the measured and calculated results are 0.0078 and 0.0059 g for the first 1 day and 6 days, respectively.

[insert Figure 6]

4 Simulated sorption isotherm measurement results and discussion

4.1 Adsorbed moisture mass evolution and judgment of the reaching equilibrium based on ISO 12571

Figure 7 shows examples of calculated distribution of the relative humidity in a specimen on the section, including the center of the model (z = 0 in Fig. 4). The target humidity was set to 75%, and the Case A condition was used for the specimen dimensions in these calculations. The distribution in an AAC specimen at 2 h after the beginning of the adsorption, in a pine specimen at 12 h, and in a OSB specimen at 58 h (when the average humidity in the section is approximately 50%) are presented in the figure.

[insert Figure 7]

The moisture distribution in the OSB was considerably larger than those in the other materials owing to the small vapor permeability. The results also show that the anisotropy of the moisture transfer properties of the pine strongly affects the moisture distribution inside; the distribution in the longitudinal direction (x-axis direction) is significantly smaller than that in the transverse direction (y-axis direction).

Figures 8–10 show the calculated evolution of the amount of adsorbed moisture. To compare the rates at which equilibrium is approached, the ratio to the equilibrium values is shown in Figs. 8 (b), 9 (b), 10 (c), and 10 (d). The effects of the material properties and target humidity are compared in Figs. 8 and 9, respectively. For the other conditions, the material properties of the concrete were used, the target humidity was set to 75%, and Case A was used for the specimen dimensions. We compared the effects of the specimen dimensions, as shown in Fig. 10. The results for the AAC and concrete under 75% humidity conditions are presented.

[insert Figure 8]
[insert Figure 9]
[insert Figure 10]

Figure 8 shows that the adsorption rate order almost corresponds to the vapor permeability order. In addition, Fig. 9 shows that the adsorption consumes more time in the high humidity range where the moisture capacity of the concrete is large. According to Fig. 10, the influences of the specimen size are significant for both materials; the adsorption rate is enlarged by dividing the specimen into small pieces (Case A).

Based on these results, the attainment of equilibrium was determined by following the criterion provided in ISO 12571. Figure 11 shows an example of the rate of the mass change per day for case C-75-A. It was assumed that the specimens were weighed at intervals of 24 h from the start of the measurement (i.e., $(m–m')/m'$, where m is the current mass of the specimen, and m' is the mass measured 1 day before). In this case, the rate of the mass change falls below 0.1% 3 days after the start of the measurement, and it is expected that the attainment of equilibrium will be judged after several days.

[insert Figure 11]

Next, Fig. 12 shows the number of days required until the attainment of equilibrium is evaluated, which was calculated under all conditions of the material, target humidity, and dimensions of the specimens considered in this study. We compared the effects of the material properties and target humidity in Fig. 12 (a) and the material properties and dimensions of the specimens in Fig. 12 (b). For the other conditions, the target humidity was set to 75%, and Case A was used for the specimen dimensions. Because it is necessary to perform three consecutive measurements of the specimen mass, several more days are required after the mass change per day falls below 0.1%. The minimum number of days required to confirm equilibrium was 3 days.

[insert Figure 12]

At relative humidities from 33% to 75%, the number of days to complete the measurement was the shortest for AAC and GB and the longest for OSB when the results under the same relative humidity and specimen dimensions were compared. In particular, the smaller the vapor permeability, the more time was consumed to complete the measurement. When the target humidity was set to 93%, the number of days until the attainment of equilibrium was judged increase significantly for AAC, pine, and OSB, because the moisture capacity of the AAC significantly increases in the high humidity range (as shown in Fig. 1), and the vapor permeability of the pine in the transverse direction and OSB is considerably small (as shown in Table 1).

Considering the effects of the specimen size (Fig. 12(b)), the number of days to complete the measurement increased significantly for materials with low density, such as pine, when the specimen volume was set to meet the ISO standard (minimum 10 g). In addition, the number of days until the end of measurement significantly depended on the specimen volume for materials with small vapor permeability, such as OSB.

As aforedescribed, the number of days until the attainment of equilibrium state is judged significantly depends on the type of material, target relative humidity, and dimensions of the specimen.

For materials such as pine and OSB, whose measurement consumes time in the entire humidity range, or AAC, which has high moisture capacity in the high humidity range, frequent mass measurement is not necessary just after the start of the experiment. In addition, for materials with low vapor permeability, such as pine and OSB, it is particularly effective to use small specimens to shorten the measurement (it is better to use specimens divided into small pieces with sufficient volume rather than a single small specimen to avoid the influence of non-uniformity of the material properties on the measurement results). For example, the time required for the experiment can be decreased by 2 and 5 days when using Case A instead of Cases B and C, respectively, when pine is utilized and by 7 and 10 days, respectively, when using OSB.

4.2 Efficiency and accuracy of the criterion to judge the attainment of equilibrium

In the previous subsection, we examined the number of days required for the measurement when the attainment of equilibrium was determined according to the criterion specified in ISO 12571. In this subsection, we further examine the efficiency and accuracy of the criterion.

4.2.1 Case of specimens with high vapor permeability

As mentioned in Section 4.1, AAC and GB, which have high vapor permeability, adsorb moisture quickly, and the attainment of equilibrium may be judged in a short period after the start of the measurement. Therefore, when ideal measurement conditions with slight external disturbance are achieved, it is expected that the time required for the measurement can be significantly reduced by determining the attainment of equilibrium from the mass measurement at time intervals below 24 h.

As an example, the rate of mass change per day calculated from the mass at an interval of 1 h ($24(m–m'')/m''$, where m'' is the specimen mass measured 1 h before the current mass measurement) was compared with that calculated from the mass at an interval of 1 d, as shown in Fig. 13. It was assumed that the AAC specimens with the Case A dimensions were exposed to air with 75% humidity. Most of the adsorption occurs within a few hours after the start of the measurement, and the rate of mass change decreases more rapidly than that calculated from the mass at an interval of 1 d; the mass change is below 0.1% at 14 h after the start of the measurement.

[insert Figure 13]

Figure 14 compares the number of days until the rate of the mass change per day calculated from the mass at an interval of 1 h is below 0.1% for all materials, target humidities, and specimen dimensions considered in this study. Based on the results, the equilibrium can be judged to be reached in 0.5 to 2 days less than when judged from the 1 day interval weighting. In particular, using AAC or GB, it takes less than a half day after the start of the measurement under 33%–75% humidity, except

in the case of AAC specimens with relatively large volumes. Therefore, it is effective to judge the attainment of the equilibrium state from the measurement results at short intervals if the external disturbance is properly decreased.

[insert Figure 14]

4.2.2 Accuracy of the criterion using the rate of the mass change

Attempts have been made to determine whether the equilibrium is reached based on a mass change rate of 0.1% in accordance with ISO 12571. However, for materials with low moisture content, such as AAC and GB, it is questionable whether a mass change of 0.1% is sufficiently small to judge the attainment of equilibrium. For example, the moisture content by mass of pine at 53% relative humidity is 0.085 kg/kg, and the 0.1% variation in the mass is small. Conversely, the moisture contents by mass of concrete and GB are 0.013 and 0.005 kg/kg, respectively, and the 0.1% variation in the mass may not be negligible compared to the moisture content of the specimen.

Figure 15 shows the days until the amount of moisture adsorbed by the specimens reaches 99% of that in the steady state as a criterion of "actual" equilibrium. Using this criterion, the time until the end of the measurement becomes longer for AAC and pine under the 93% humidity condition and for concrete and OSB under all humidity conditions (as shown in Fig. 15 (a)) than when the attainment of the equilibrium is judged from 1 h interval weighting (Fig. 14). In addition, it is more time consuming for pine and OSB when the specimen size is larger (as shown in Fig. 15 (b)). Especially for OSB, the time until the end of the measurement becomes longer than when the attainment of the equilibrium is judged from 1 day interval weighting (Fig. 12), because moisture adsorption consumes considerable time, especially in the region close to the steady state where the moisture distribution in the specimens is small when the vapor permeability of a material is small or the specimen volume is large. For example, when the target humidity is 75% and the specimen size is that of Case A (case OSB-75-A), it takes 6 days before the attainment of equilibrium is judged based on ISO 12571 (shown in Fig. 12); however, the amount of adsorbed moisture is approximately 97% of that in the actual equilibrium state. When the target humidity is changed to 93% and the specimen size to that of Case C (case OSB-93-C), the amount of adsorbed moisture when the equilibrium state is judged to be reached based on ISO 12571 is approximately 95% and 89% of the value in the actual equilibrium state, respectively. Therefore, there is a considerable risk of underestimation of the moisture content depending on the target humidity and specimen size.

Therefore, for materials with low moisture content and vapor permeability or for specimens with large volume, judgment of reaching the equilibrium state from a mass change per day of 0.1% is likely to cause underestimation of the moisture content during the sorption process. It is necessary to use a more stringent criterion based on the hygric properties of the material. For example, for case OSB-75-

A, the attainment of equilibrium should be determined from a mass change per day of 0.04% to obtain the moisture content after 99% of the adsorption is completed. In addition, dividing the specimens into small pieces enhances the uniformity of the moisture distribution in the specimens and decreases the risk of underestimation.

[insert Figure 15]

5 Limitation

5.1 Employed physical model

In this study, we used a common physical model and hygrothermal properties. The limitations caused by these choices are as follows.

We used a standard hygrothermal model, in which moisture transfer was described according to Fick's law of diffusion. However, slow absorption that is not subject to Fickian diffusion has been observed in several building materials (Wadsö, 1994; Saeidpour and Wadsö, 2015). This phenomenon can be a reason for the deviation between the measurement and calculation results (Fig. 6), along with inaccuracy of the moisture properties employed in the simulations. The calculation results fairly reproduce the trend of the measurement results, enabling us to examine possible improvements and risks of errors in our study. However, in the future, more advanced physical models should be developed and validated with various ranges of variables. Thus far, physical models that can account for non-Fickian behavior are not readily available for a wide variety of building materials; however, those for wooden and fiber materials have been developed (Krabbenhoft, 2004; Korjenic and Bednar, 2011; Challansonnex et al., 2019). In the future, such models will be necessary to propose the measurement duration and errors of the adsorption isotherms effectively, along with investigation into this problematic phenomenon.

5.2 Calculation cases and conditions

5.2.1 Representativeness of specimen dimensions

In this study, the three or four levels of the dimensions of the specimens were chosen for all types of building materials to clarify the effects of material properties on the rate of reaching equilibrium. However, the suitable range of the specimens' dimensions for the tests should differ depending on the material homogeneity. For example, the comparison of the absorption rates with relatively large dimensions will be useful for materials like concrete, which is highly heterogeneous due to the existence of aggregates. ISO 12571 does not specify sampling methods for such materials, but specimens for material property measurements should be sufficiently large to ensure that they contain all composite materials with average volume fraction. In particular, concrete has an interfacial transition zone that has a high porosity compared with that of the bulk cement paste between the

aggregates and cement paste (Scrivener and Nemati, 1996; Basheer et al., 2005). Therefore, the representative volume is related to the aggregate size. For example, Wu et al. (2015) demonstrated that a sample volume of $7d^3$, where d is the maximum aggregate size, could be considered as the representative volume in determining the desorption isotherm of concrete. Based on their study, when d is 10 mm, the mass of a specimen should be more than 15.4 g, and the edges should be longer than 19.1 mm when it is cubic, which are greater than the sizes specified in Cases A and C in this study as well as in the ISO standard. Studies with dimensions suitable for each material should be conducted for more practical application in the future.

Furthermore, ISO 12571 mentioned that a specimen can be crushed when the results are not affected. This strategy may significantly reduce the test time and should be investigated in subsequent research. Notably, general hygrothermal models cannot reproduce the absorption behaviors of such small specimens. For example, the moisture diffusion in the gap between particles cannot easily be considered. Moreover, the effects of non-Fickian behavior will not be negligible in such small specimens because it is considered to take place on short-length scales (Wadsö, 1994; Saeidpour and Wadsö, 2015). Therefore, the use of crashed samples should be investigated while revealing these phenomena and performing corresponding physical modeling.

5.2.2 Disturbance during the experiments

In this study, we assumed ideal experimental conditions with slight external disturbance as the first step of the examination. However, the effects of such disturbances, including unstable temperature, insufficient humidity control, exposure of the specimens to air in the laboratory, and air exchange in the desiccator during weighting, must be further examined.

6 Conclusion

In this study, we investigated the possible improvement and risks of errors of the standardized sorption isotherm measurement method using a three-dimensional calculation model of the heat and moisture transfer in the material. We simulated the sorption isotherm measurement process specified in ISO 12571, using values of the hygrothermal properties of typical building materials listed in an international database. Concrete was chosen as an example of cement-based materials, AAC (autoclaved aerated concrete) and GB (gypsum board) as those of board materials, and pine and OSB as those of wooden materials, and the adsorption rates were compared. The results can be summarized as follows.

- For materials with low vapor permeability and/or high moisture capacity in certain humidity regions, such as AAC, pine, and OSB, the sorption process consumes considerable time; thus, the mass measurement of the specimens to confirm equilibrium can be postponed for several days to a week from the start of the experiment, whereas ISO 12571 specifies that only the mass of a

specimen should be periodically measured until it is in equilibrium with the environment.

- Typical board materials, such as AAC and GB, characterized by high vapor permeability (on the order of 10^{-11} kg/(m·s·Pa)) and low moisture capacity (<0.02 m^3/m^3 at a humidity of 75%) especially in the low humidity region, adsorb moisture quickly, and the attainment of equilibrium may be judged in a short period after the start of the measurement. Therefore, when ideal measurement conditions with slight disturbance are achieved, equilibrium attainment can be determined from hourly mass measurements, which can significantly reduce the time required for measurement.
- During sorption measurement using materials with low moisture content and vapor permeability, the criterion of a mass change rate of 0.1% per day leads to underestimation of approximately 10% equilibrium moisture content at most under the tested calculation conditions. More stringent criteria depending on the hygric properties of the material should be used to decrease measurement errors, e.g., a mass increase of 0.01% per day can be a good criterion when a sufficient apparatus is available. In addition, dividing a specimen into small pieces is effective in decreasing the risk of underestimation.

Notably, large volumes of materials with low densities such as pine are required when the volume is set to enable the specimen mass to meet the ISO standard (minimum 10 g). In addition, for materials with low vapor permeability, such as typical wooden materials, the number of days to complete the measurement significantly depends on the specimen volume. For such materials, it is particularly effective to divide the specimen into smaller pieces to shorten the measurement by up to 40%–50% under the tested calculation conditions.

References

Asphaug SK, Time B and Kvande T (2021) Hygrothermal simulations of thermally insulated basement envelopes - Importance of boundary conditions below grade. *Building and Environment* 199: 107920.

ASHRAE (2002) A Thermal and Moisture Transport Property Database for Common Building and Insulating Materials: Final Report from ASHRAE Research Project 1018-RP.

ASTM C1498 - 04a (2016) Standard Test Method for Hygroscopic Sorption Isotherms of Building Materials.

Banfill FP (2021) Hygrothermal properties of Scottish building stone and mortar: data for Scottish masonry materials. *Materials and Structure* 54: 167.

Bao J et al. (2020) Coupled effects of sustained compressive loading and freeze–thaw cycles on water penetration into concrete. *Structural Concrete* 22: E944-54.

Basheer L, Basheer PAM and Long AE (2005) Influence of coarse aggregate on the permeation, durability and the microstructure characteristics of ordinary Portland cement concrete.

463 *Construction and Building Materials* 19: 682-90
464 Bauklimatik Dresden, DELPHIN. Available at: http://bauklimatik-dresden.de/delphin/ (Accessed 8
465 July 2021).
466 Bui R, Labat M and Aubert J-E (2017) Comparison of the saturated salt solution and the dynamic
467 vapor sorption techniques based on the measured sorption isotherm of barley straw. *Construction*
468 *and Building Materials* 141: 140-51.
469 Challansonnex A, Casalinho J and Perré P (2019) Non-Fickian diffusion in biosourced materials:
470 Experimental determination of the memory function using minute samples. *Construction and*
471 *Building Materials* 224: 560-71
472 Chen H-Y and Chen C (2014) Equilibrium relative humidity method used to determine the sorption
473 isotherm of autoclaved aerated concrete. *Building and Environment* 81: 427-35.
474 Delgado JMPQ et al. (2010) A critical review of hygrothermal models used in porous building
475 materials. *Journal of Porous Media* 13: 221-34.
476 Eckert E and Drake RJ (1987) *Analysis of heat and mass transfer.* New York: Hemisphere Publishing.
477 EN 15026:2007 (2007) Hygrothermal performance of building components and building elements -
478 Assessment of moisture transfer by numerical simulation.
479 Fabbri A and McGregor (2017) Impact of the determination of the sorption-desorption curves on the
480 prediction of the hemp concrete hygrothermal behaviour. *Construction and Building Materials*
481 157: 108-16.
482 Fabbri A et al. (2017) Effect of temperature on the sorption curves of earthen materials. *Materials and*
483 *Structures* 50: 253.
484 Feng C et al. (2013) Validating various measures to accelerate the static gravimetric sorption isotherm
485 determination. *Building and Environment* 69: 64-71.
486 Fraunhofer IBP, WUFI (en). Available at: https://wufi.de/en/ (Accessed 7 July 2021).
487 ISO 12571 (2013) Hygrothermal performance of building materials and products: determination of
488 hygroscopic sorption properties.
489 JIS A 1475:2004 (2004) *Method of test for hygroscopic sorption properties of building materials.*
490 Korjenic A and Bednar T (2011) Developing a model for fibrous building materials. *Energy and*
491 *Buildings* 43: 3189-99.
492 Krabbenhøft K (2004) *Moisture Transport in Wood: A Study of Physical-Mathematical Models and*
493 *their Numerical Implementation.* Lyngby: Technical University of Denmark.
494 Kumaran MK (1996) *IEA Annex 24, Final Report, Vol. 3, Task 3: Material Properties.* Leuven:
495 Laboratorium Boufysica, Department Burgerlijke Bouwkunde, KU Leuven.
496 Kumaran MK (2006) A thermal and moisture property database for common building and insulation
497 materials. *ASHRAE Transactions* 112: 485-497.
498 Künzel H M (1995) *Simultaneous heat and moisture transport in building components: one- and two-*

499 *dimensional calculation using simple parameters.* Dissertation, Fraunhofer IRB, Germany.
500 Luan H, Wu J and Pan J (2020) Saline water absorption behavior and critical saturation degree of
501 recycled aggregate concrete during freeze-thaw cycles. *Construction and Building Materials* 258:
502 119640.
503 Martínez-Marino S et al. (2021) Simulation and validation of indoor temperatures and relative
504 humidity in multi-zone buildings under occupancy conditions using multi-objective calibration.
505 *Building and Environment* 200: 107973.
506 Ma S et al. (2020) Mechanical properties and water absorption of cement composites with various
507 fineness and contents of waste brick powder from C&D waste. *Cement and Concrete Composites*
508 114: 103758.
509 McGregor F et al. (2014) The moisture buffering capacity of unfired clay masonry. *Building and*
510 *Environment* 82: 599-607.
511 Nakajima M et al. (2020) Field survey of the relationship between environmental conditions and algal
512 growth on exterior walls. *Building and Environment* 169: 106575.
513 Parracha JL et al. (2021) Effects of hygrothermal, UV and SO2 accelerated ageing on the durability of
514 ETICS in urban environments. *Building and Environment* 204: 10815.
515 Peuhkuri RH, Rode C and Hansen KK (2005) Effect of method, step size and drying temperature on
516 sorption isotherms. In: *7th Nordic Symposium on Building Physics.* Reykjavík, Iceland, 13-15 June
517 2005, pp. 31-38.
518 Promis G et al. (2019) Temperature-dependent sorption models for mass transfer throughout bio-based
519 building materials. *Construction and Building Materials* 197: 513-25.
520 Rode C and Hansen KK (2011) Hysteresis and temperature dependency of moisture sorption - new
521 measurements. In: *9th Nordic Symposium on Building Physics.* Tampere, Finland, 29 May–2 June
522 2011, pp.647-54.
523 Saeidpour M and Wadsö L (2015) Evidence for anomalous water vapor sorption kinetics in cement
524 based materials. *Cement and Concrete Research* 70: 60-66.
525 Scrivener LL and Nemati KM (1996) The percolation of pore space in the cement paste/aggregate
526 interfacial zone of concrete. *Cement and Concrete Research* 26: 35-40.
527 Sakiyama NRM et al. (2021) Hygrothermal performance of a new aerogel-based insulating render
528 through weathering: Impact on building energy efficiency. *Building and Environment* 202: 108004.
529 Shi L et al. (2018) Analysis of moisture buffering effect of straw-based board in civil defence shelters
530 by field measurements and numerical simulations. *Building and Environment* 143: 366-77.
531 Tada S and Watanabe K (2005) Dynamic determination of sorption isotherm of cementbased materials.
532 *Cement and Concrete Research* 35: 2271-77.
533 Wadsö L (1994) Describing non-Fickian water-vapour sorption in wood. *Journal of Materials Science*
534 29: 2367-72.

Wang Y et al. (2019) Water absorption and chloride diffusivity of concrete under the coupling effect of uniaxial compressive load and freeze–thaw cycles. *Construction and Building Materials* 209: 566-76.

Wan H et al. (2021) Optimal moisture buffering thickness of the hygroscopic material layer: Modeling and derivation. *Building and Environment* 205: 108257.

Woloszyn M et al. (2009) The effect of combining a relative-humidity-sensitive ventilation system with the moisture-buffering capacity of materials on indoor climate and energy efficiency of buildings. *Building and Environment* 44: 515-24.

Wu Q et al. (2015) Representative volume element estimation for desorption isotherm of concrete with sliced samples. *Cement and Concrete Research* 76: 1-9.

Yamada K et al. (2020) Investigation on the deterioration mechanism of tuff stones used for the exteriors at the former Koshien Hotel. *E3S Web of Conferences* 172: 20008.

Yang L, Liu G, Gao D and Zhang C (2021) Experimental study on water absorption of unsaturated concrete: w/c ratio, coarse aggregate and saturation degree. *Construction and Building Materials* 272: 121945.

Zhang K and Richman R (2020) Variability in moisture sorption isotherms of plywood and oriented strand board with accelerated ageing. *Canadian Journal of Civil Engineering* 48: 812–18.

Zhang K and Richman R (2021) Wood sheathing durability from moisture sorption isotherm variability due to age and temperature. *Construction and Building Materials* 273: 121672.

Zhang P et al. (2017) Influence of freeze-thaw cycles on capillary absorption and chloride penetration into concrete. *Cement and Concrete Research* 100: 60-7.

Zhang X et al. (2016) Combined effects of sorption hysteresis and its temperature dependency on wood materials and building enclosures - Part I: Measurements for model validation. *Building and Environment* 106: 143-54.

Zhao P et al. (2019) Conservation of disappearing traditional manufacturing process for Chinese grey brick: Field survey and laboratory study. *Construction and Building Materials* 212: 531-40.

Lines: fitted curves; markers: provided values

Water content [m^3/m^3]

0.12
0.10
0.08
0.06
0.04
0.02
0.00

Concrete
AAC
GB
Pine
OSB

0.0
0.2
0.4
0.6
0.8
1.0

Relative humidity

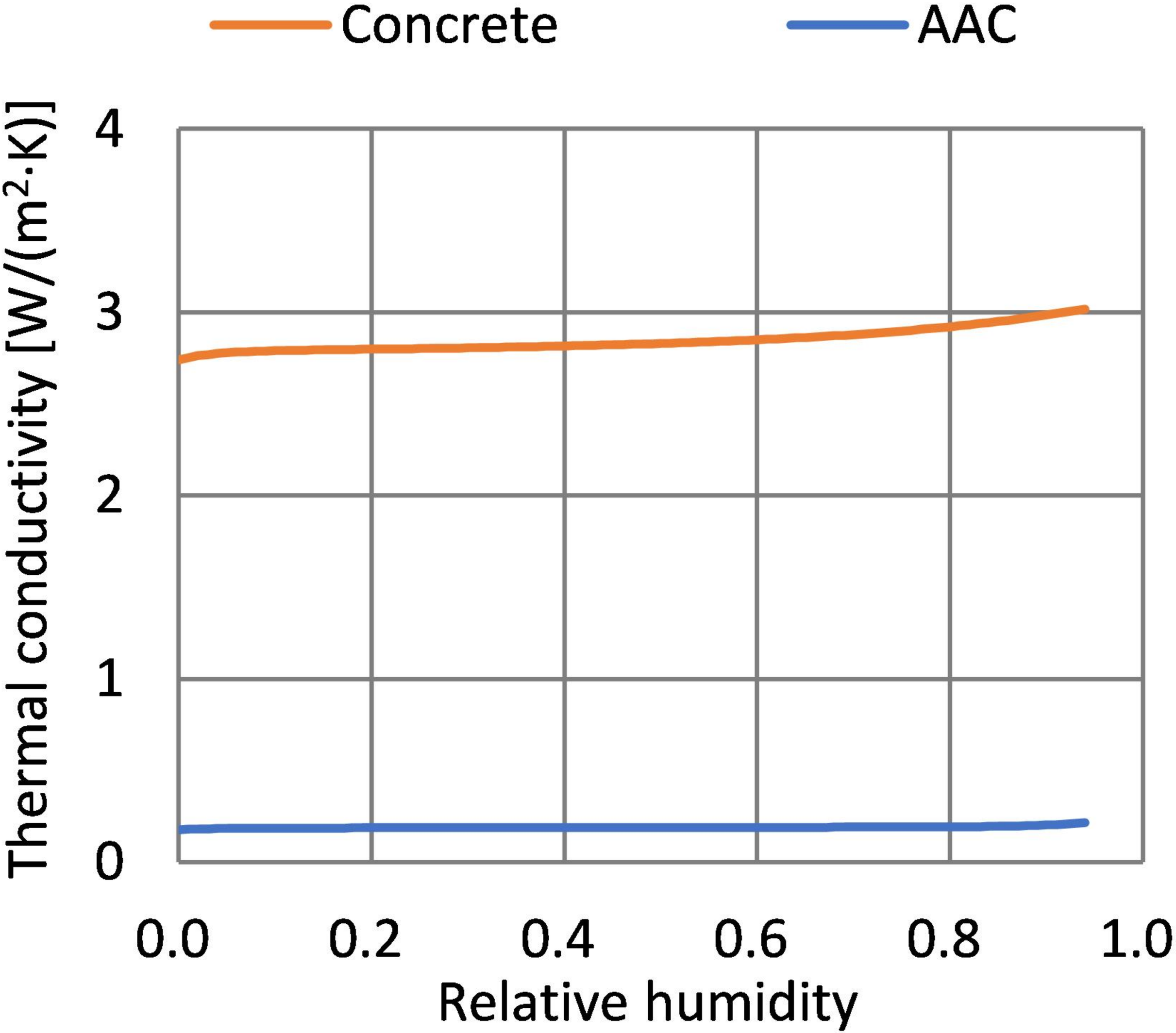
Concrete
AAC
Thermal conductivity [W/(m².K)]
4
3
2
1
0
0.0
0.2
0.4
0.6
0.8
1.0
Relative humidity

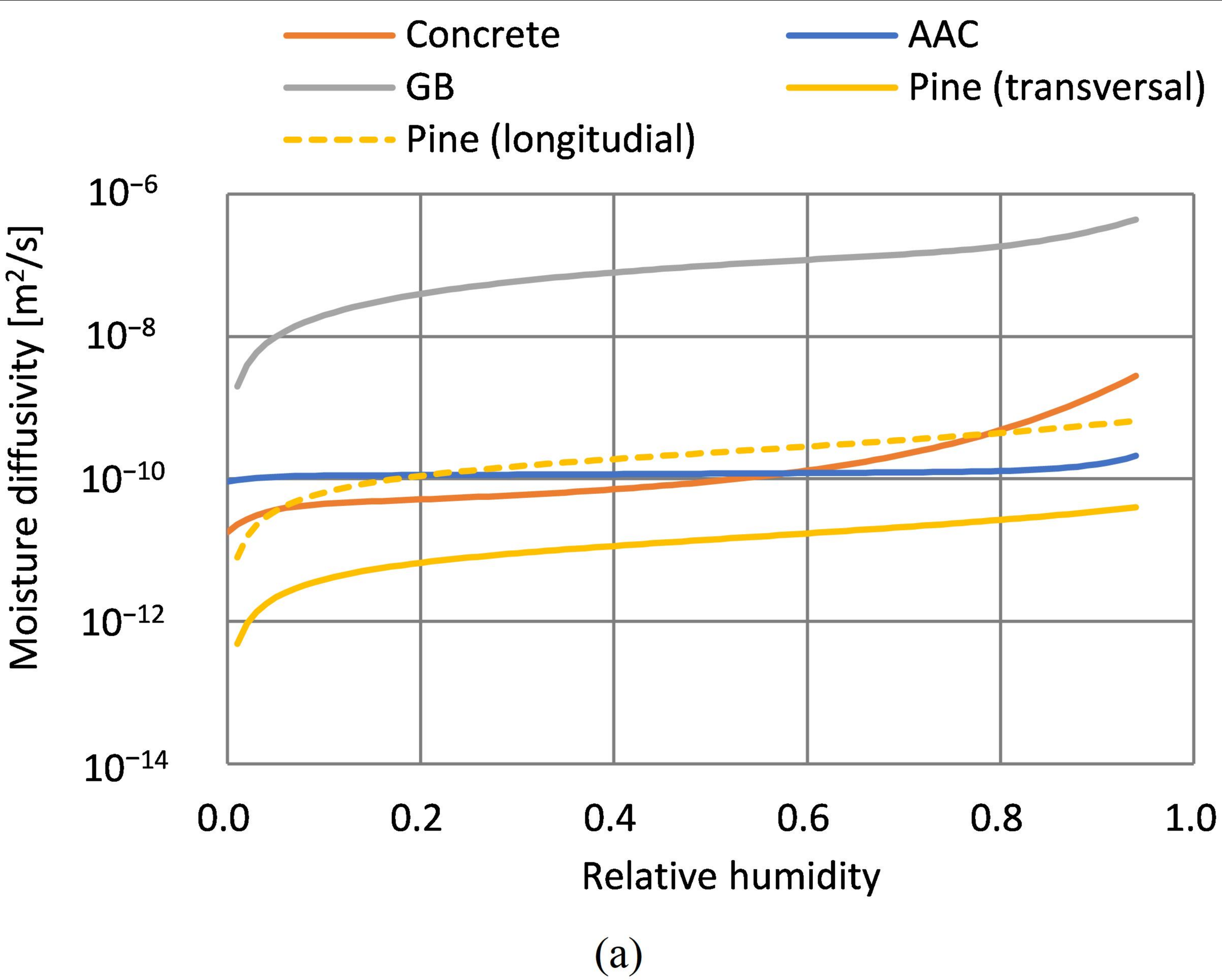
Concrete
AAC
GB
Pine (transversal)
Pine (longitudial)
Moisture diffusivity [m²/s]
10⁻⁶
10⁻⁸
10⁻¹⁰
10⁻¹²
10⁻¹⁴
0.0
0.2
0.4
0.6
0.8
1.0
Relative humidity

(a)

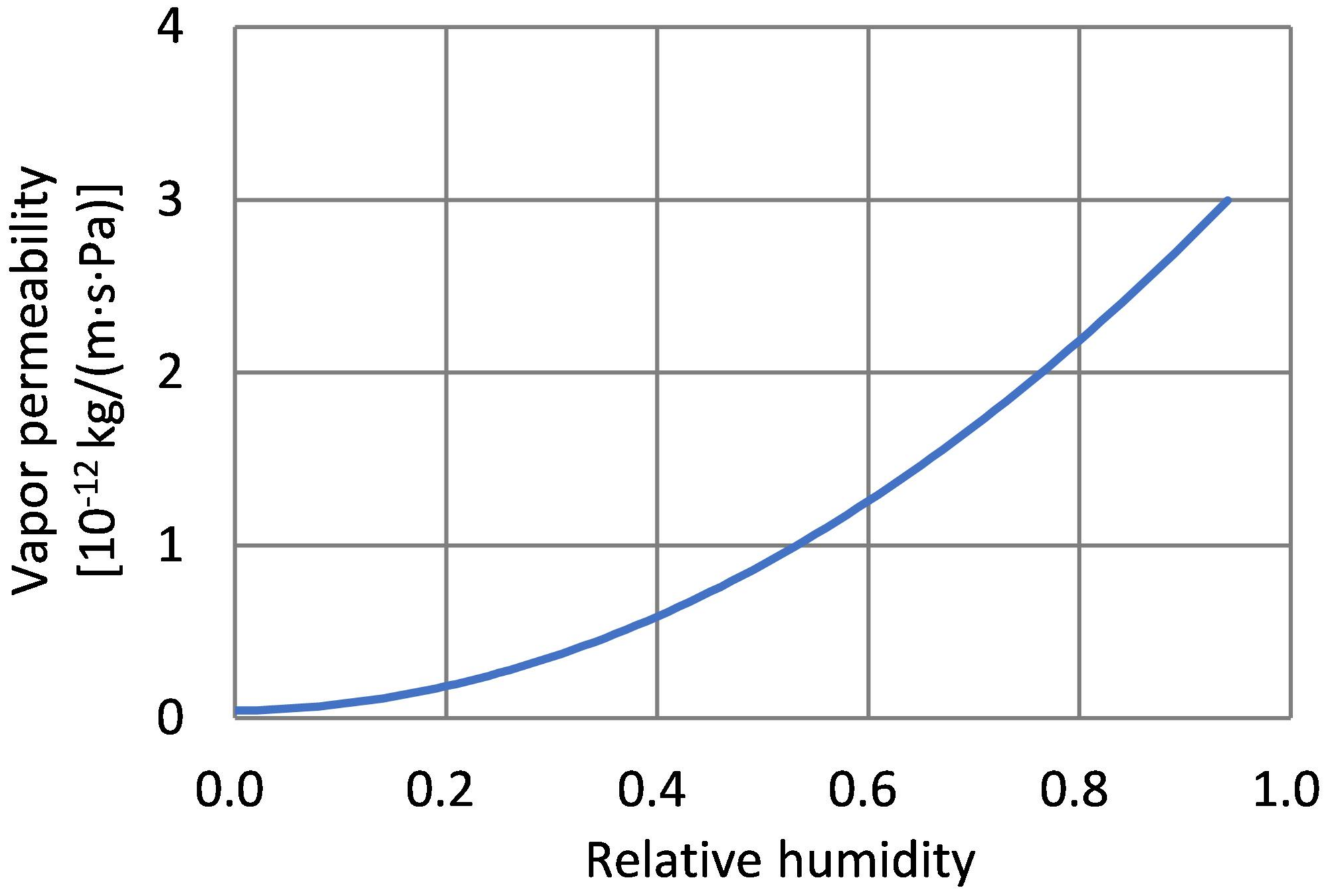
Vapor permeability
[10⁻¹² kg/(m·s·Pa)]
4
3
2
1
0
0.0
0.2
0.4
0.6
0.8
1.0
Relative humidity

(b)

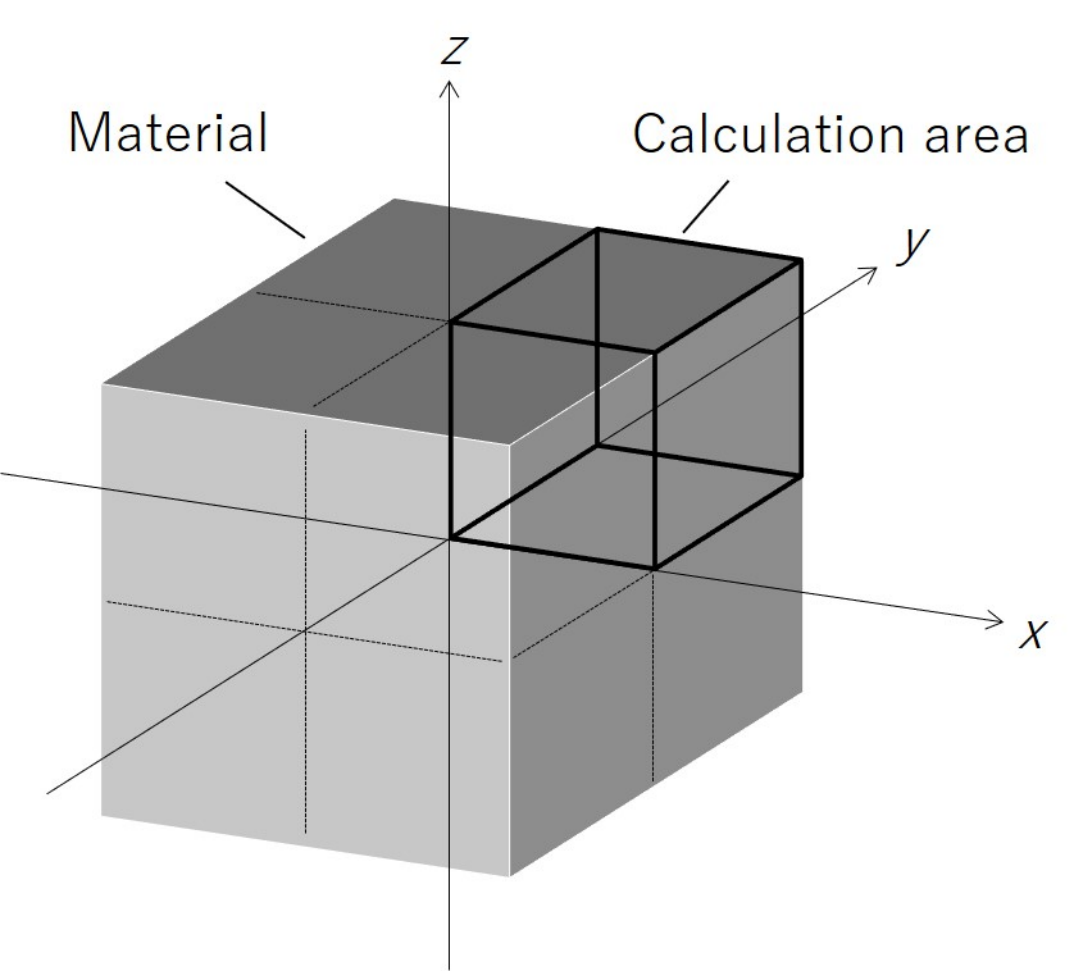
z
Material
Calculation area
y
x

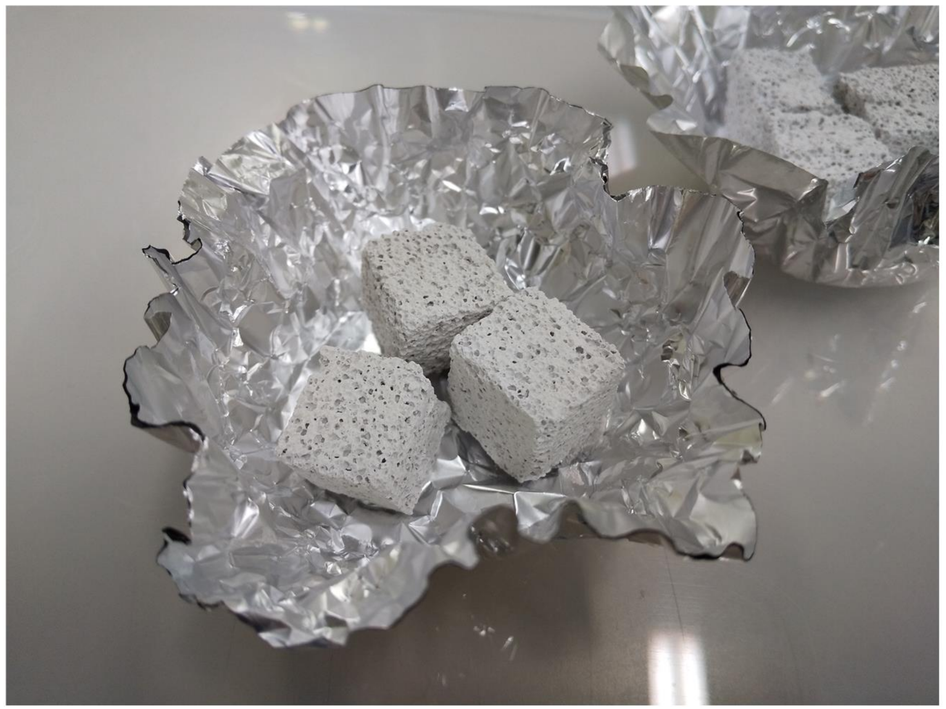

(a)

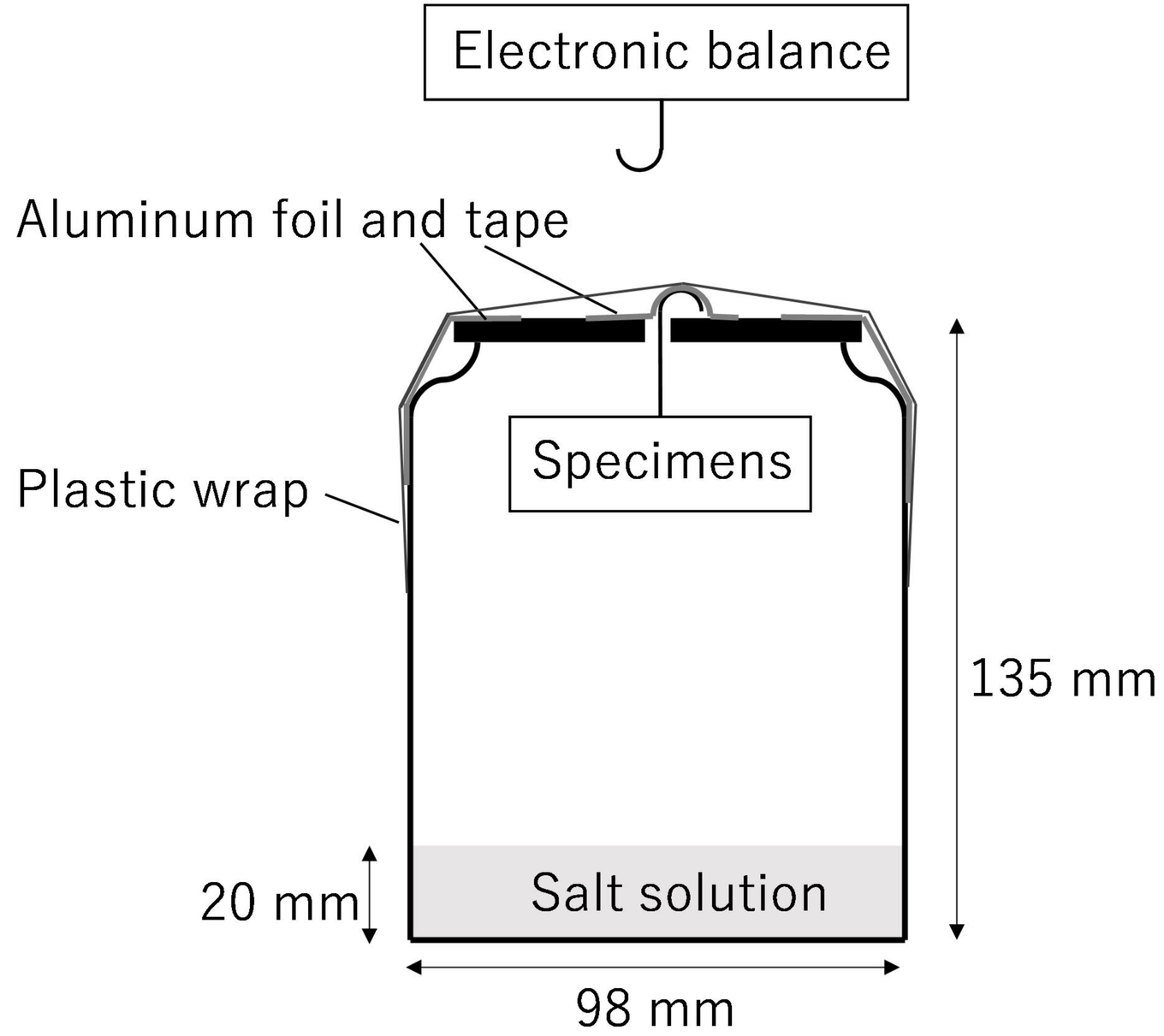
Electronic balance
Aluminum foil and tape
Plastic wrap
Specimens
135 mm
20 mm
Salt solution
98 mm

(b)

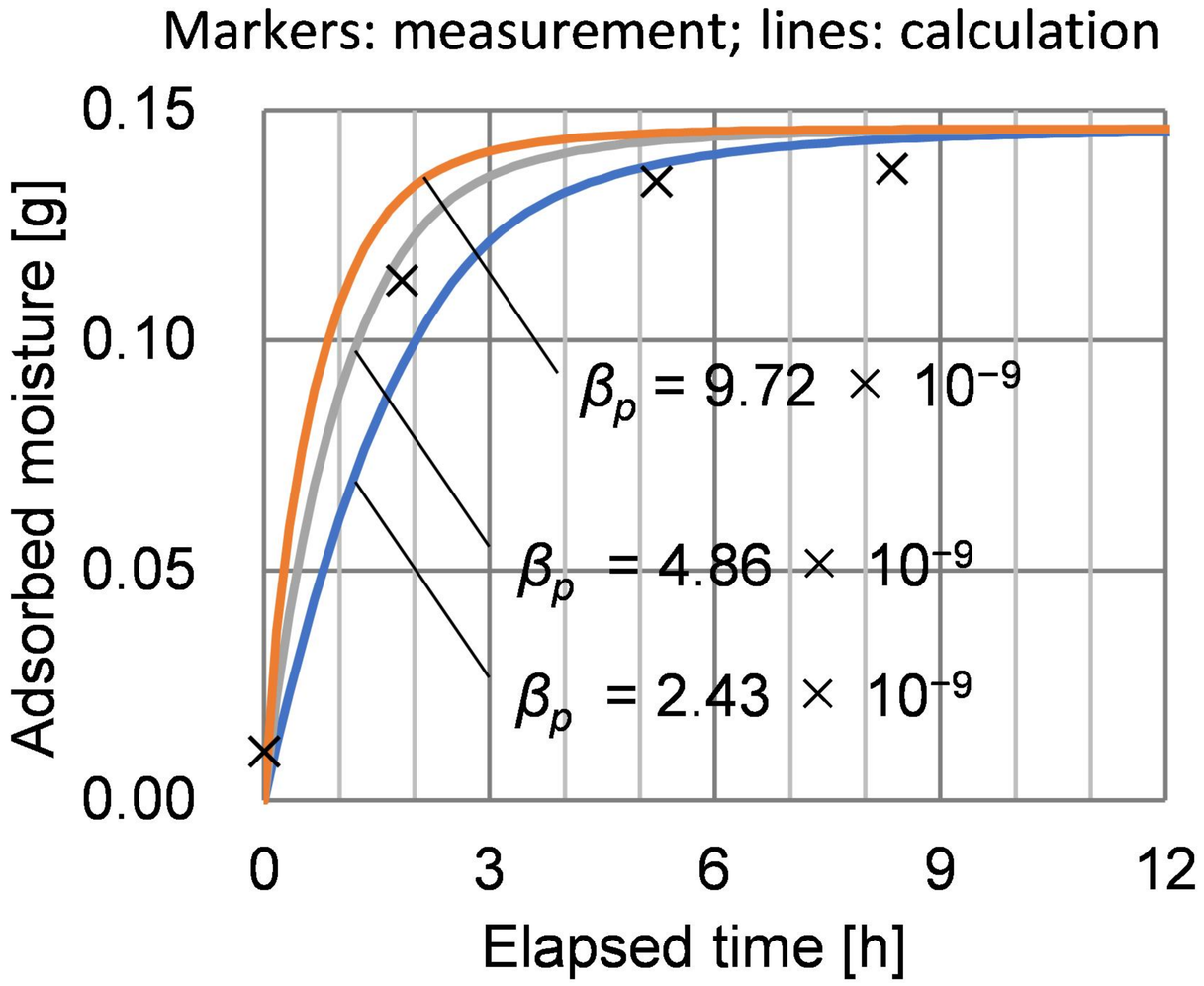
Markers: measurement; lines: calculation
0.15
0.10
0.05
0.00
Adsorbed moisture [g]
β_p = 9.72 × 10⁻⁹
β_p = 4.86 × 10⁻⁹
β_p = 2.43 × 10⁻⁹
0
3
6
9
12
Elapsed time [h]

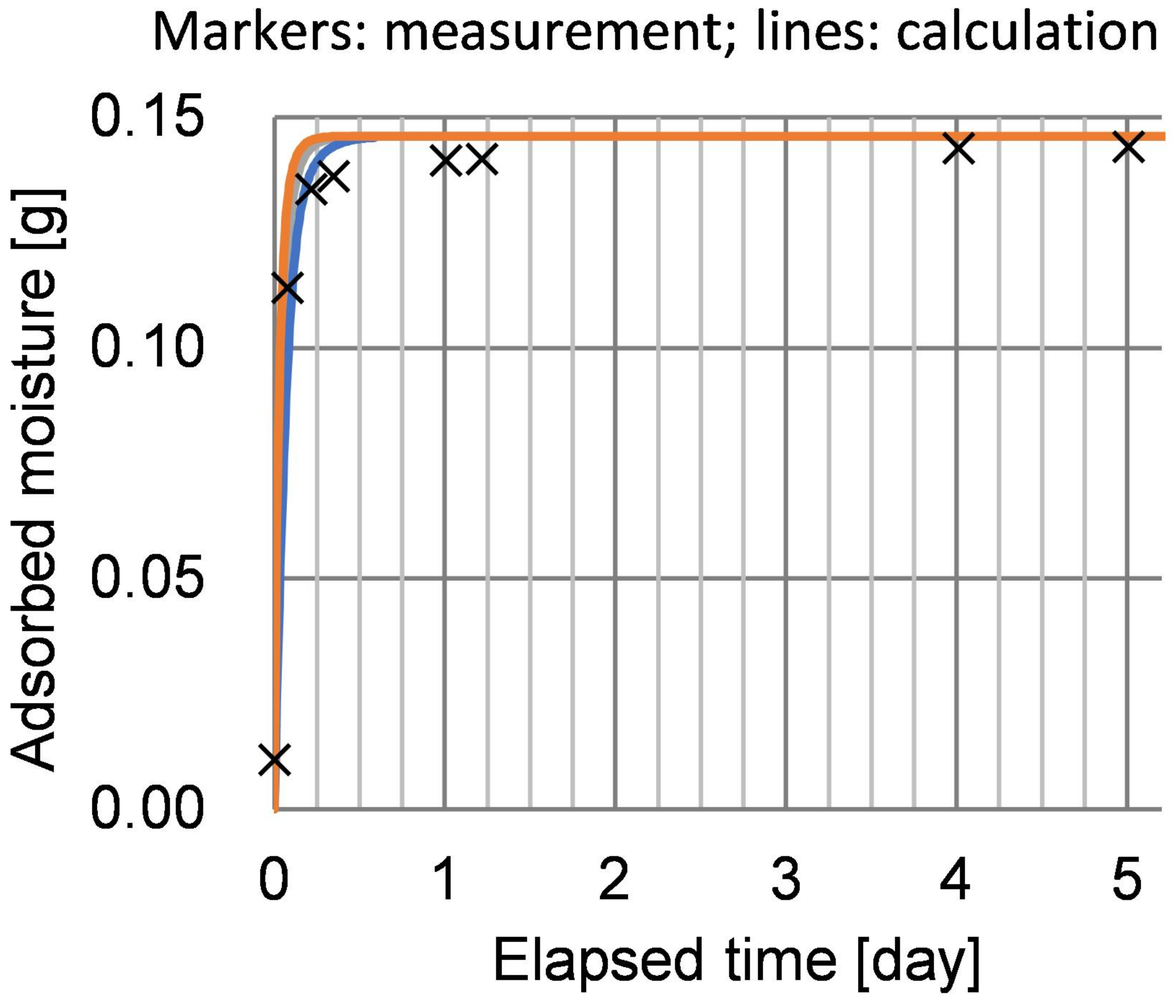
Markers: measurement; lines: calculation
0.15
0.10
0.05
0.00
Adsorbed moisture [g]
0
1
2
3
4
5
Elapsed time [day]

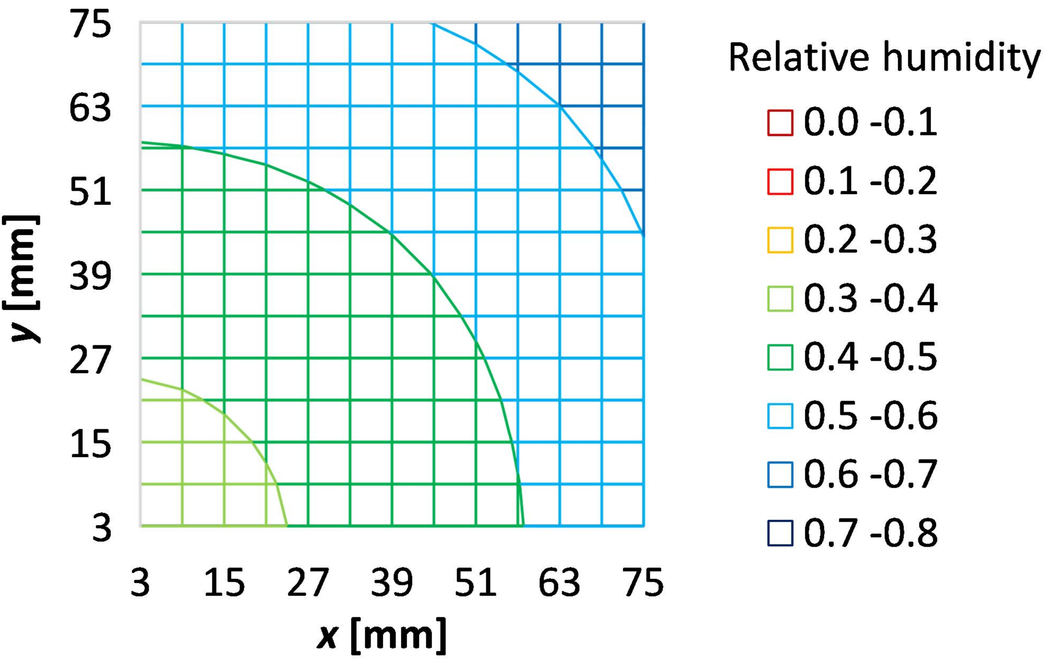
75
63
51
39
27
15
3
y [mm]
3 15 27 39 51 63 75
x [mm]
Relative humidity
0.0 -0.1
0.1 -0.2
0.2 -0.3
0.3 -0.4
0.4 -0.5
0.5 -0.6
0.6 -0.7
0.7 -0.8

(a)

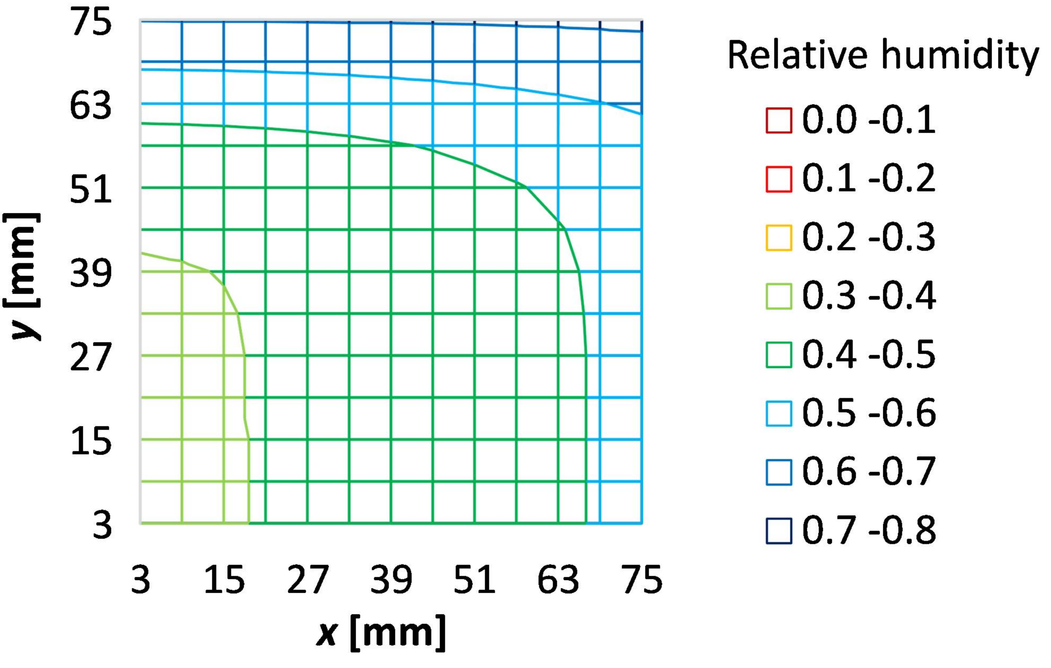
75
63
51
39
27
15
3
y [mm]
3 15 27 39 51 63 75
x [mm]
Relative humidity
0.0 -0.1
0.1 -0.2
0.2 -0.3
0.3 -0.4
0.4 -0.5
0.5 -0.6
0.6 -0.7
0.7 -0.8

(b)

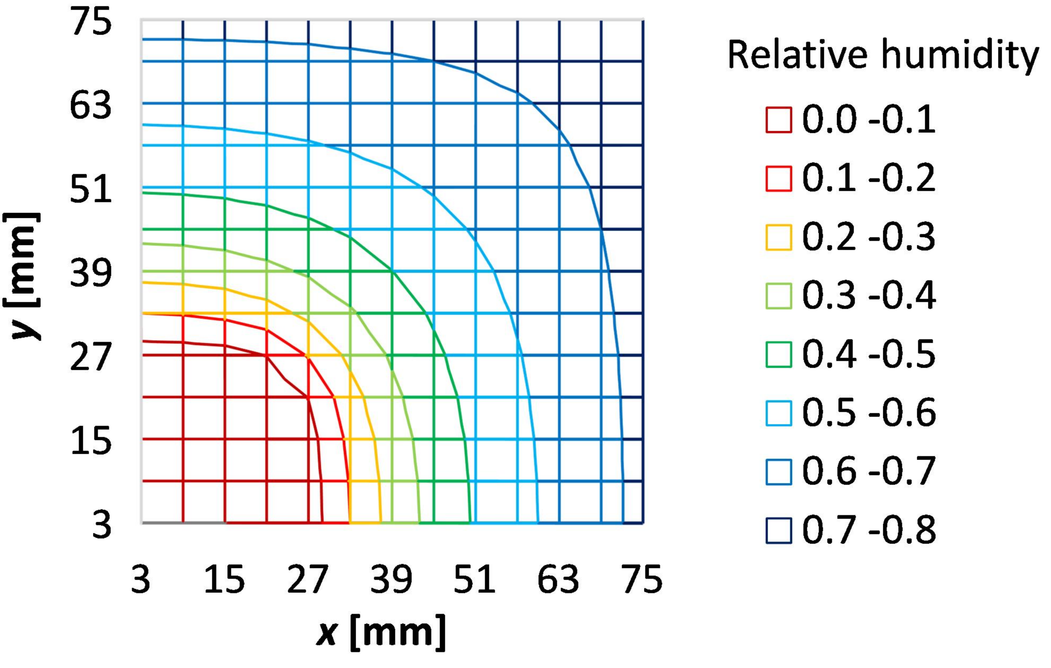
75
63
51
39
27
15
3
y [mm]
3 15 27 39 51 63 75
x [mm]
Relative humidity
0.0 -0.1
0.1 -0.2
0.2 -0.3
0.3 -0.4
0.4 -0.5
0.5 -0.6
0.6 -0.7
0.7 -0.8

(c)

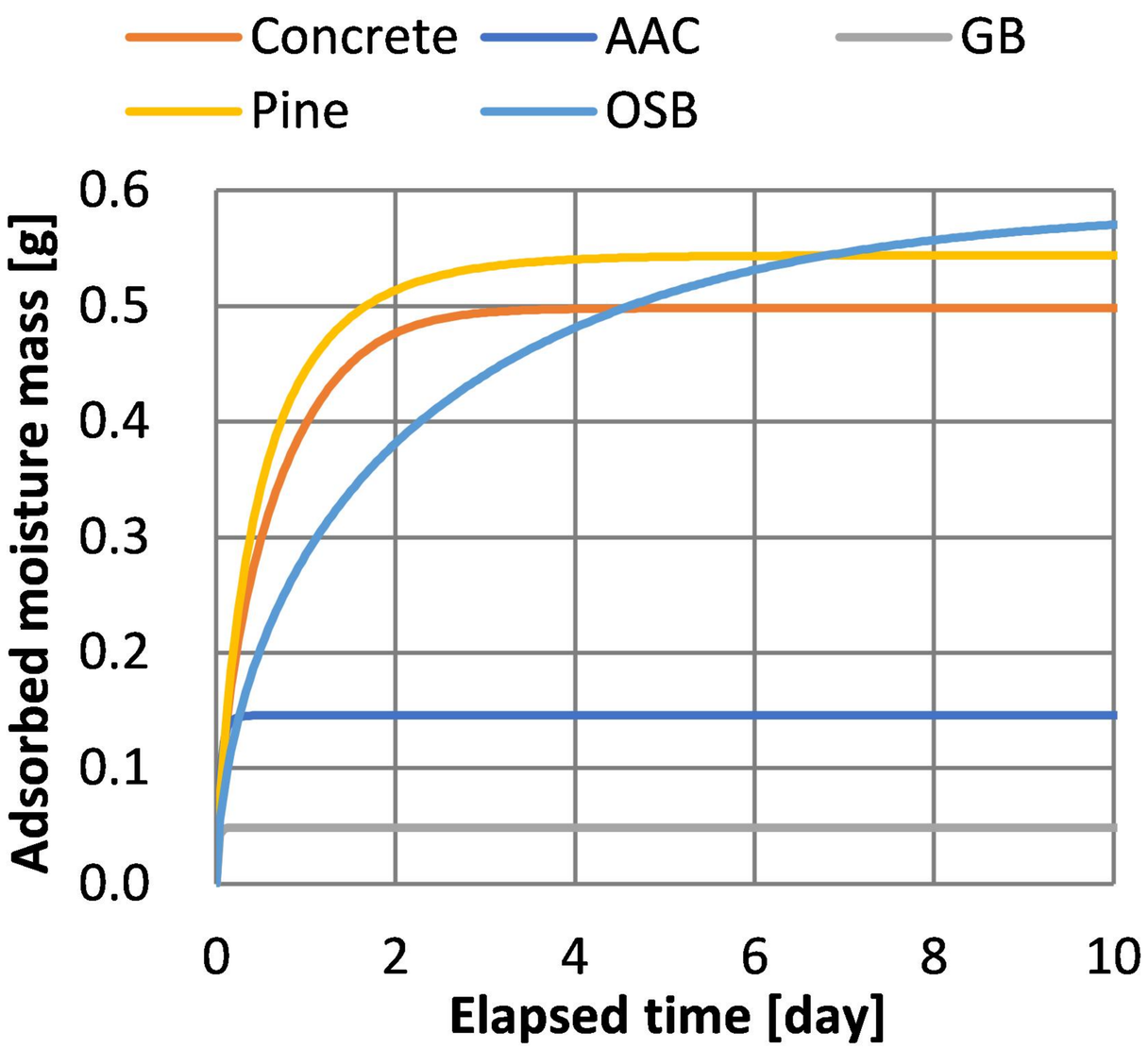
Concrete
AAC
GB
Pine
OSB
Adsorbed moisture mass [g]
0.0
0.1
0.2
0.3
0.4
0.5
0.6
0
2
4
6
8
10
Elapsed time [day]

(a)

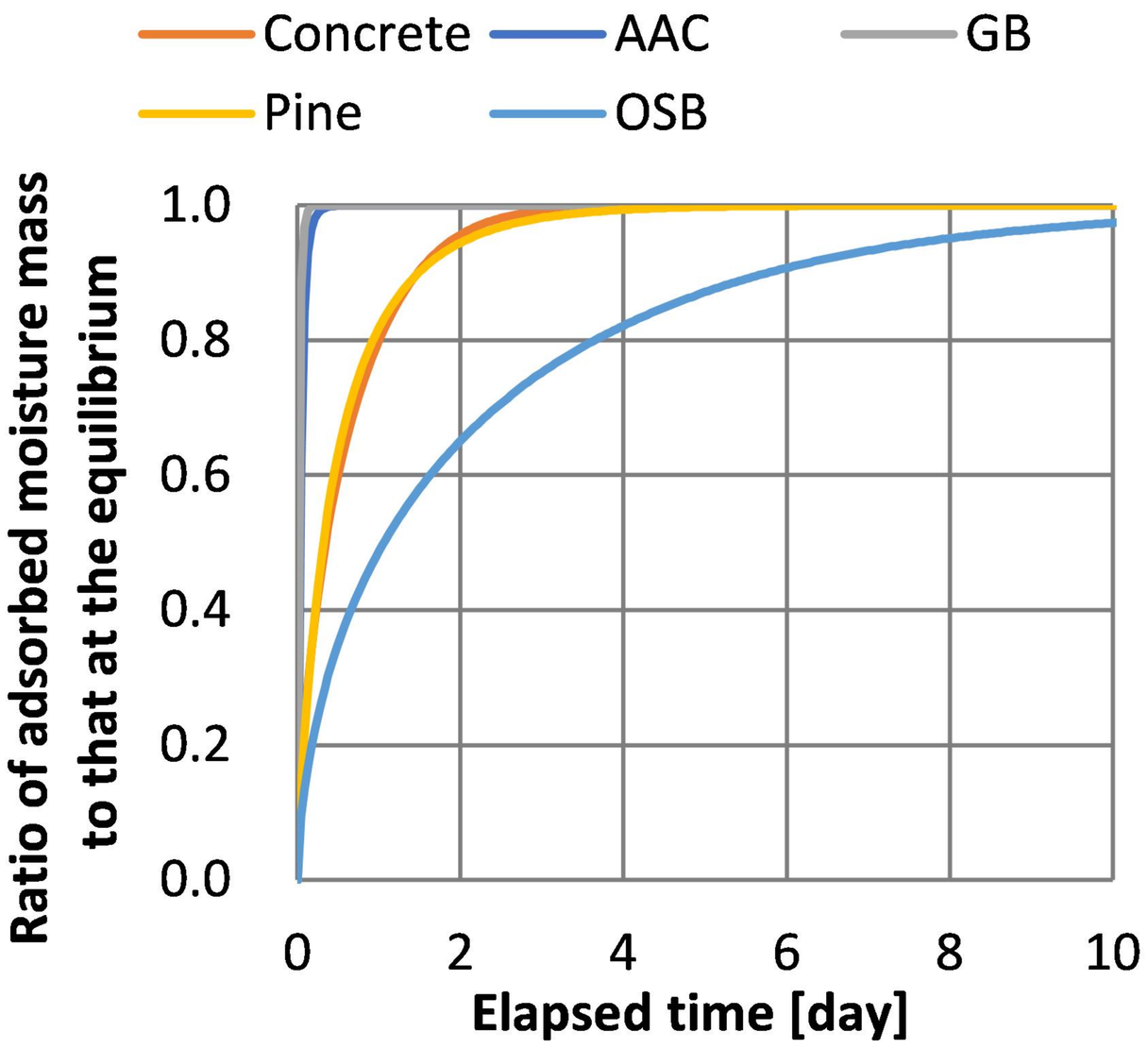
Concrete
AAC
GB
Pine
OSB
Ratio of adsorbed moisture mass to that at the equilibrium
0.0
0.2
0.4
0.6
0.8
1.0
0
2
4
6
8
10
Elapsed time [day]

(b)

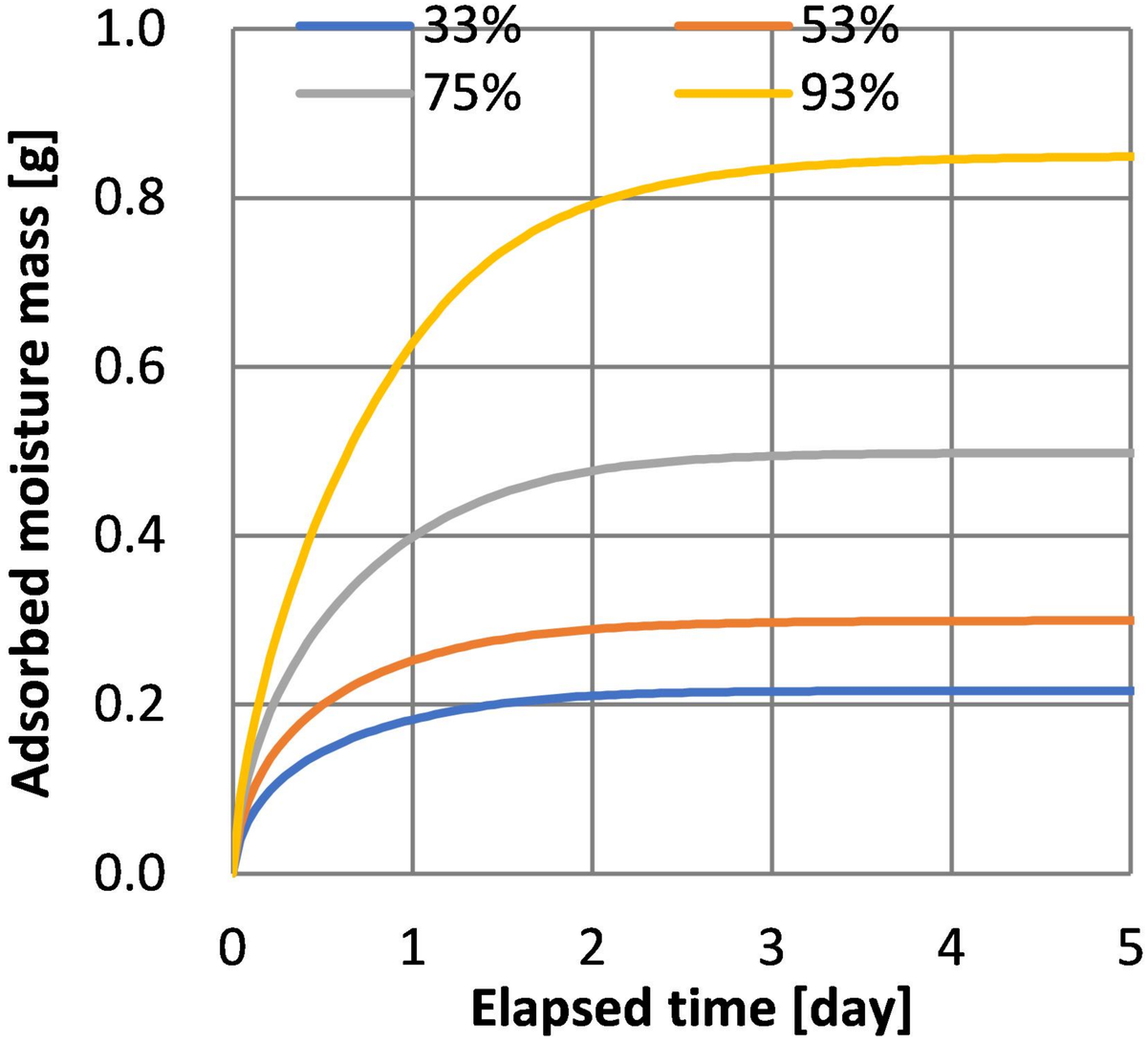
33%
53%
75%
93%
1.0
0.8
0.6
0.4
0.2
0.0
Adsorbed moisture mass [g]
0
1
2
3
4
5
Elapsed time [day]

(a)

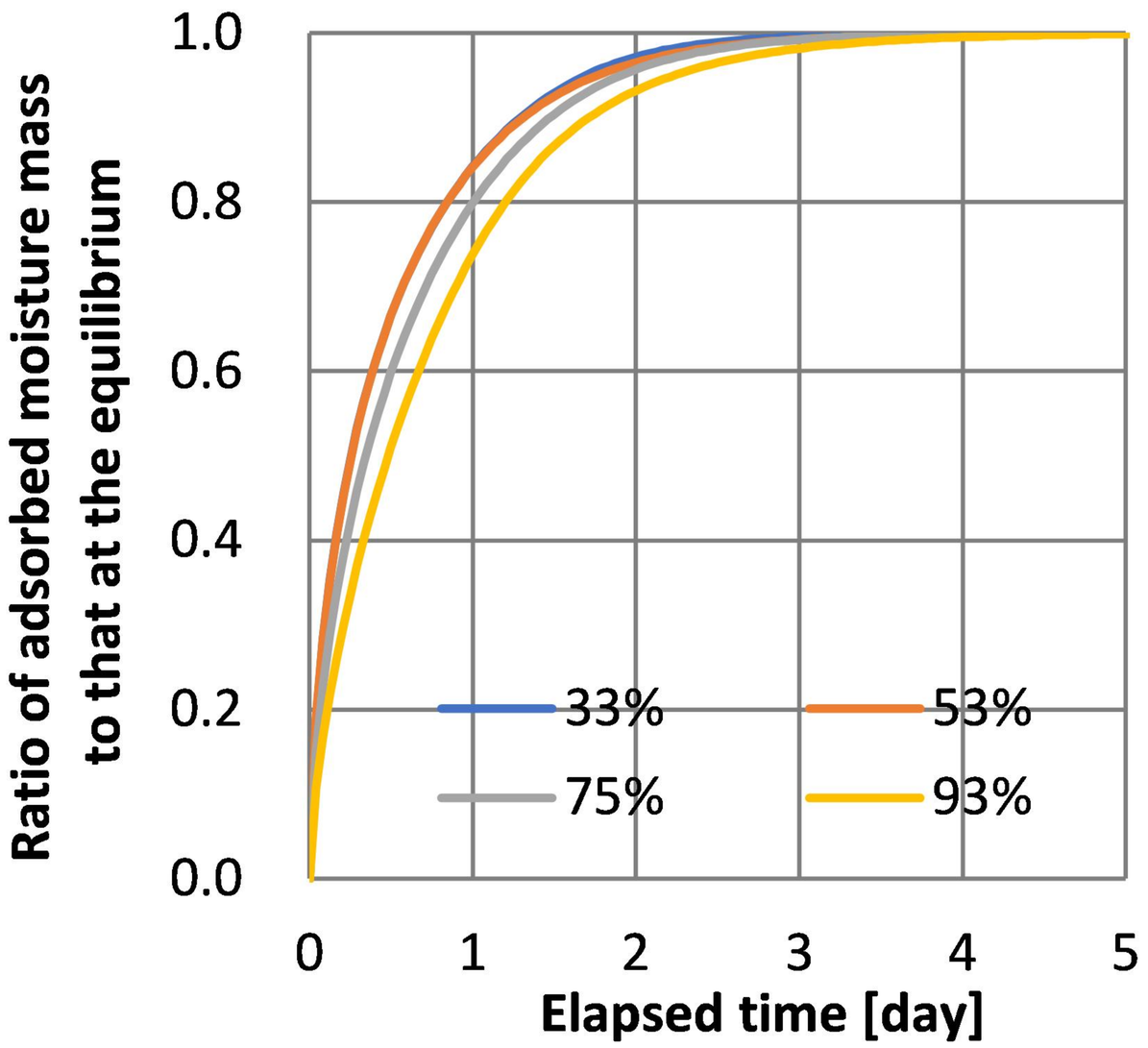
1.0
0.8
0.6
0.4
0.2
0.0
Ratio of adsorbed moisture mass to that at the equilibrium
33%
53%
75%
93%
0
1
2
3
4
5
Elapsed time [day]

(b)

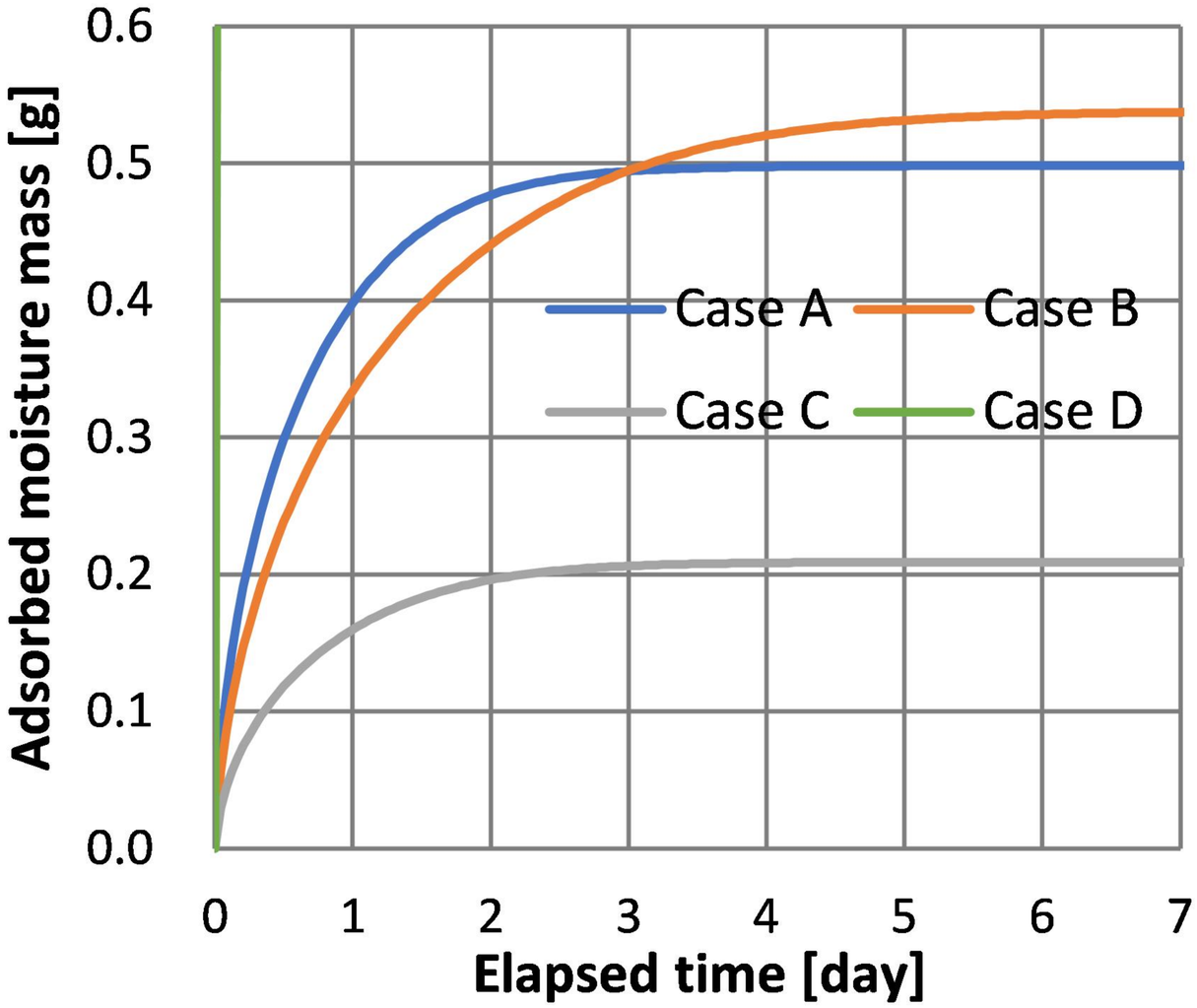
Adsorbed moisture mass [g]
0.6
0.5
0.4
0.3
0.2
0.1
0.0
0
1
2
3
4
5
6
7
Elapsed time [day]
Case A
Case B
Case C
Case D

(a)

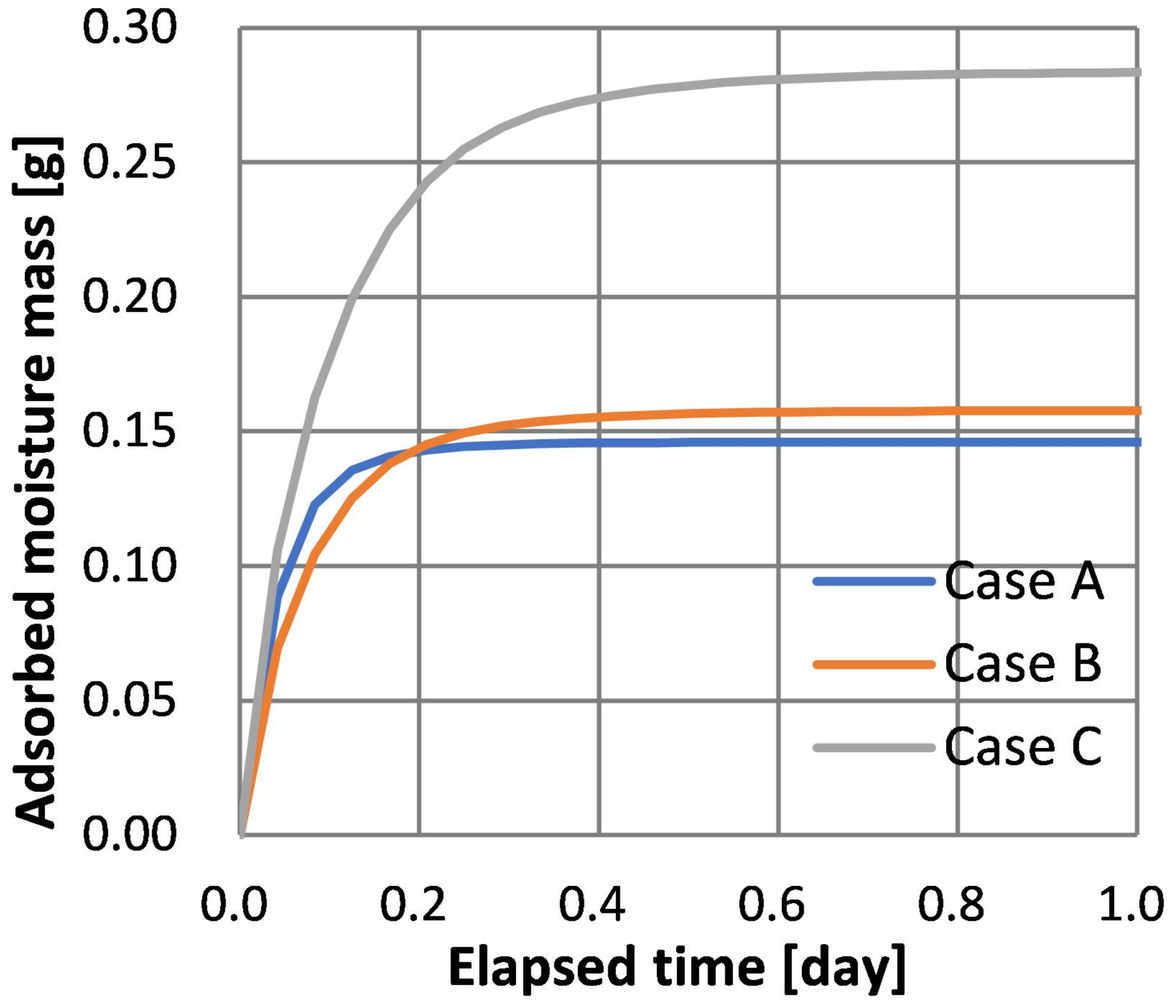
Adsorbed moisture mass [g]
0.30
0.25
0.20
0.15
0.10
0.05
0.00
0.0
0.2
0.4
0.6
0.8
1.0
Elapsed time [day]
Case A
Case B
Case C

(b)

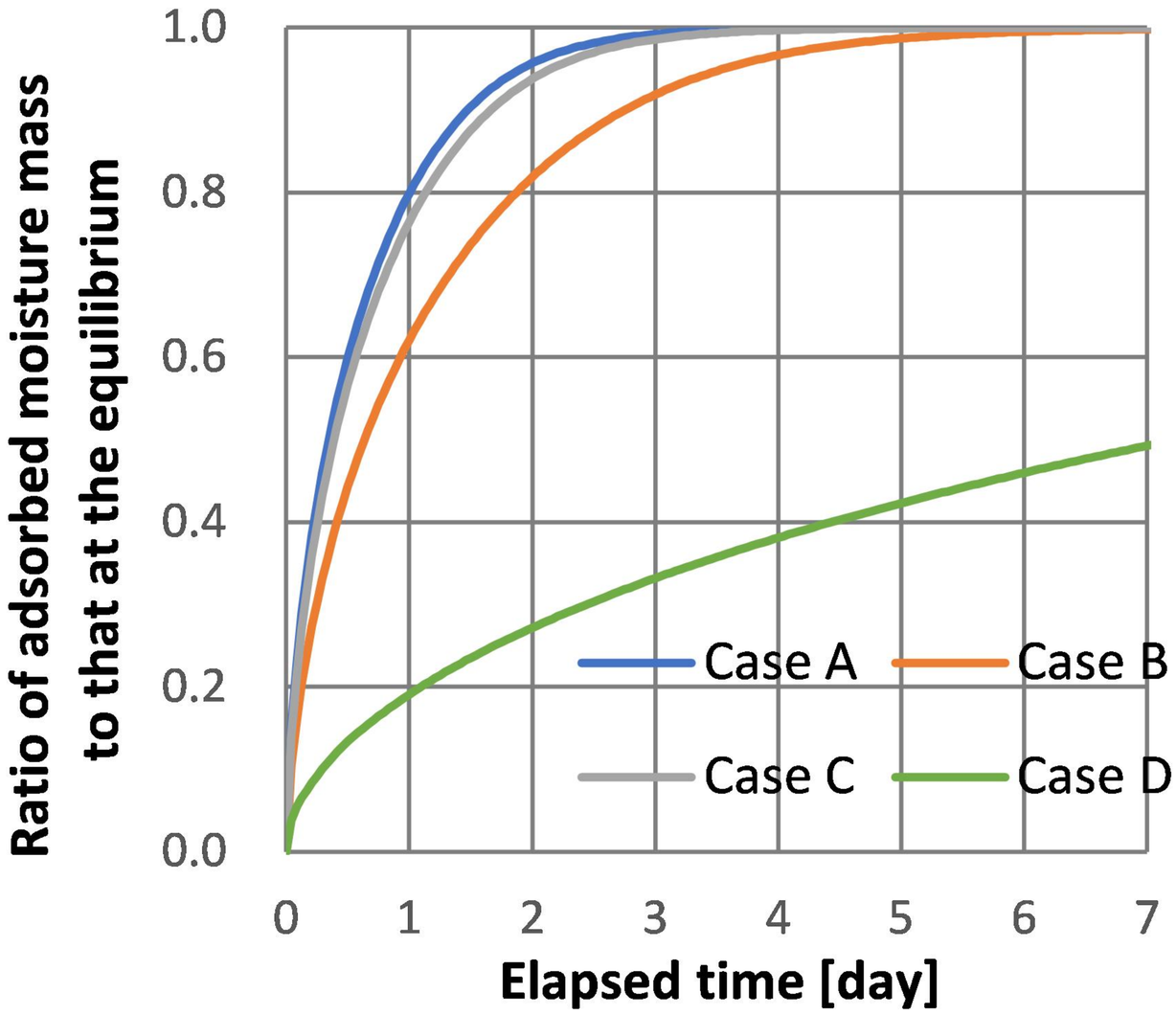
Ratio of adsorbed moisture mass to that at the equilibrium
1.0
0.8
0.6
0.4
0.2
0.0
0
1
2
3
4
5
6
7
Elapsed time [day]
Case A
Case B
Case C
Case D

(c)

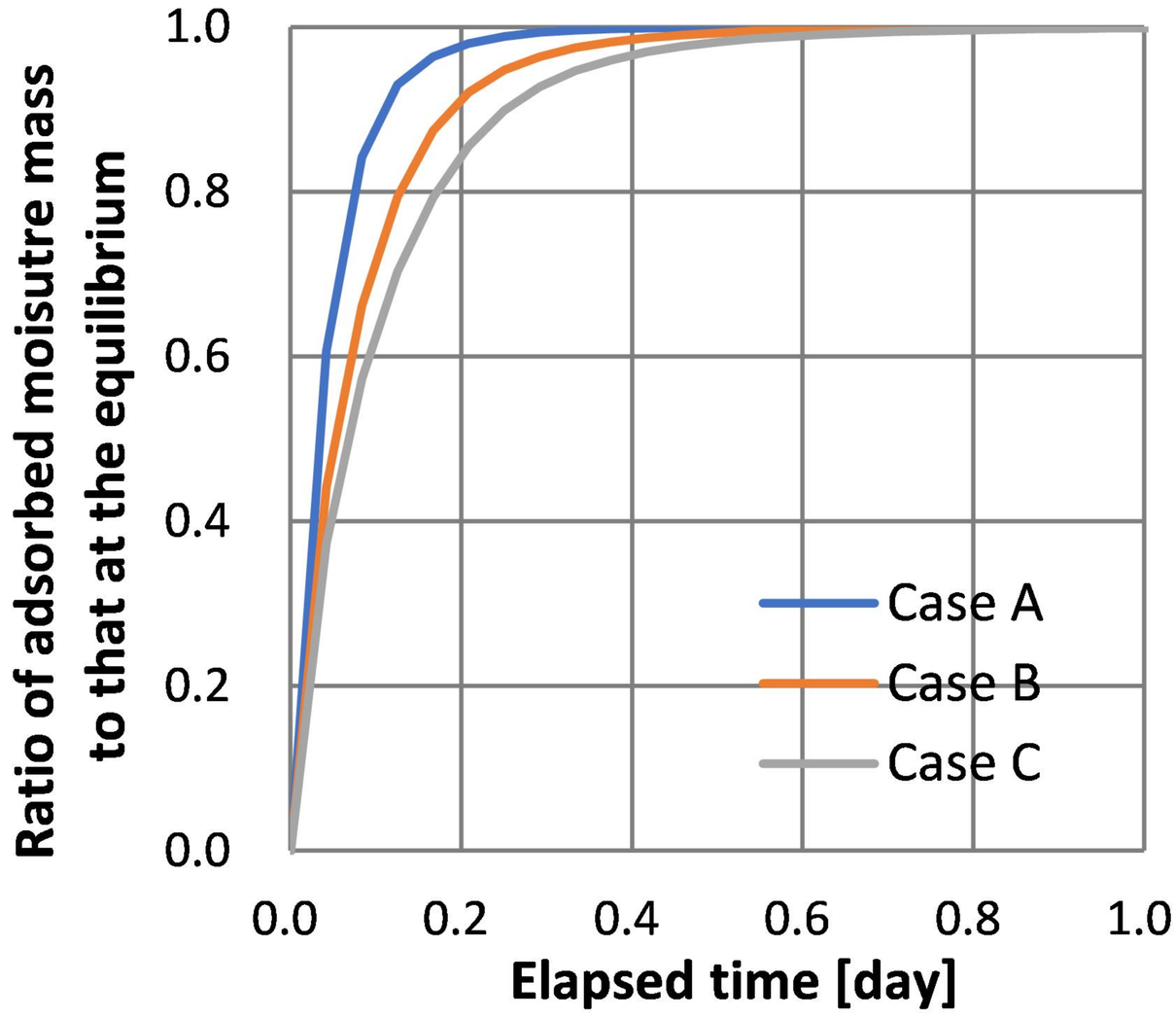
Ratio of adsorbed moisutre mass to that at the equilibrium
1.0
0.8
0.6
0.4
0.2
0.0
0.0
0.2
0.4
0.6
0.8
1.0
Elapsed time [day]
Case A
Case B
Case C

(d)

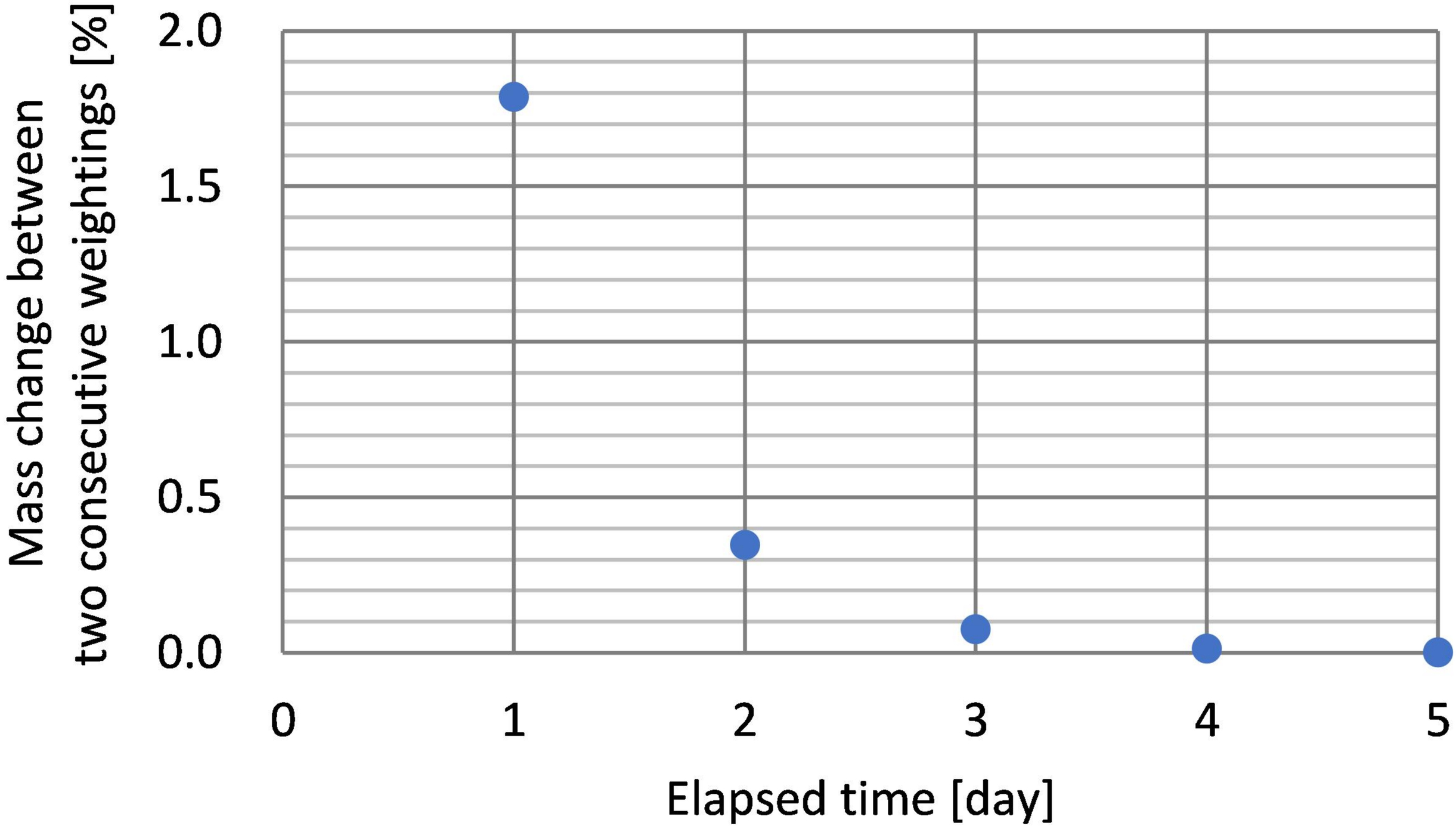
Mass change between two consecutive weightings [%]
2.0
1.5
1.0
0.5
0.0
0
1
2
3
4
5
Elapsed time [day]

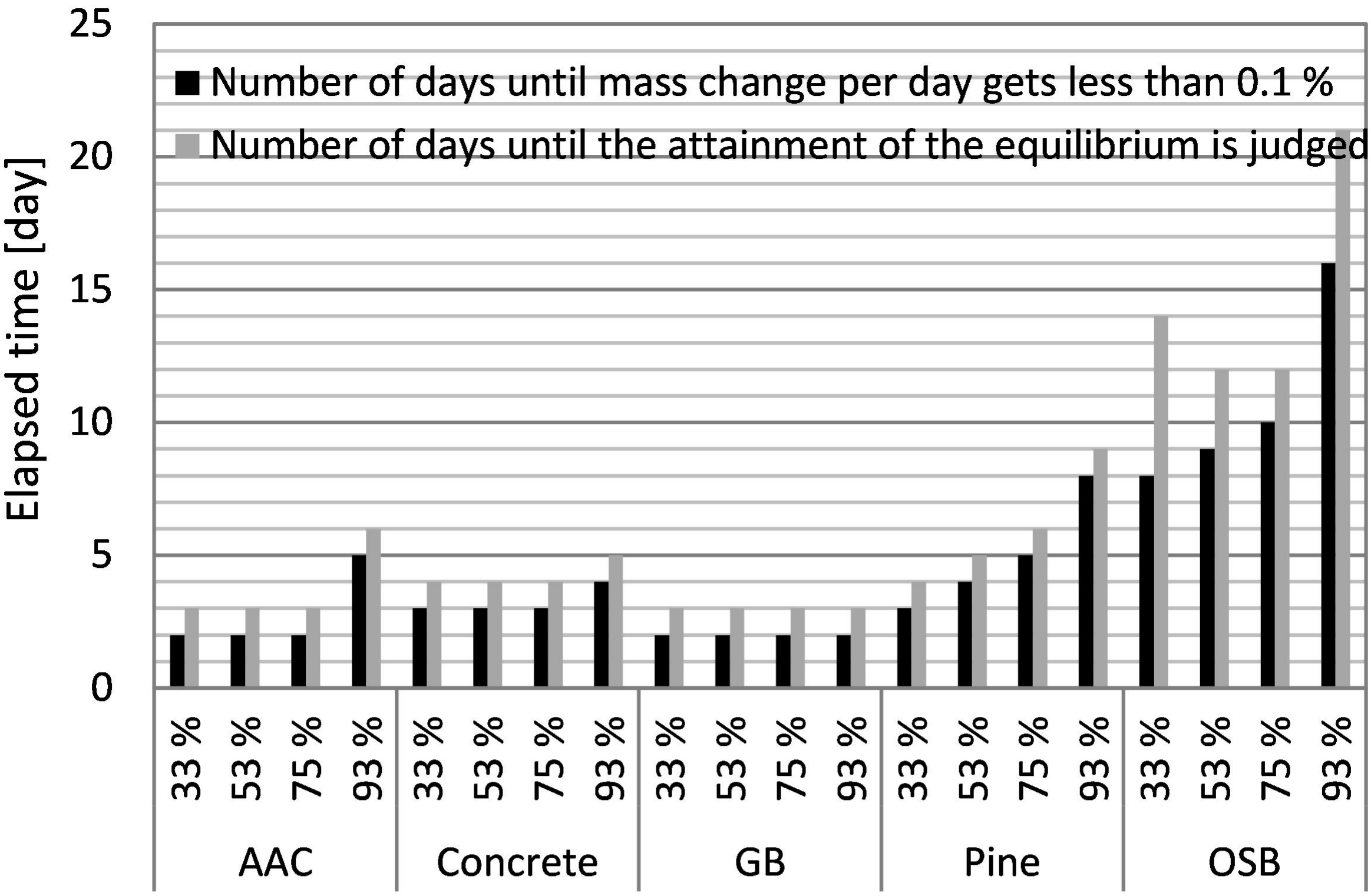
Number of days until mass change per day gets less than 0.1 %
Number of days until the attainment of the equilibrium is judged
Elapsed time [day]
0
5
10
15
20
25
33 %
53 %
75 %
93 %
AAC
Concrete
GB
Pine
OSB

(a)

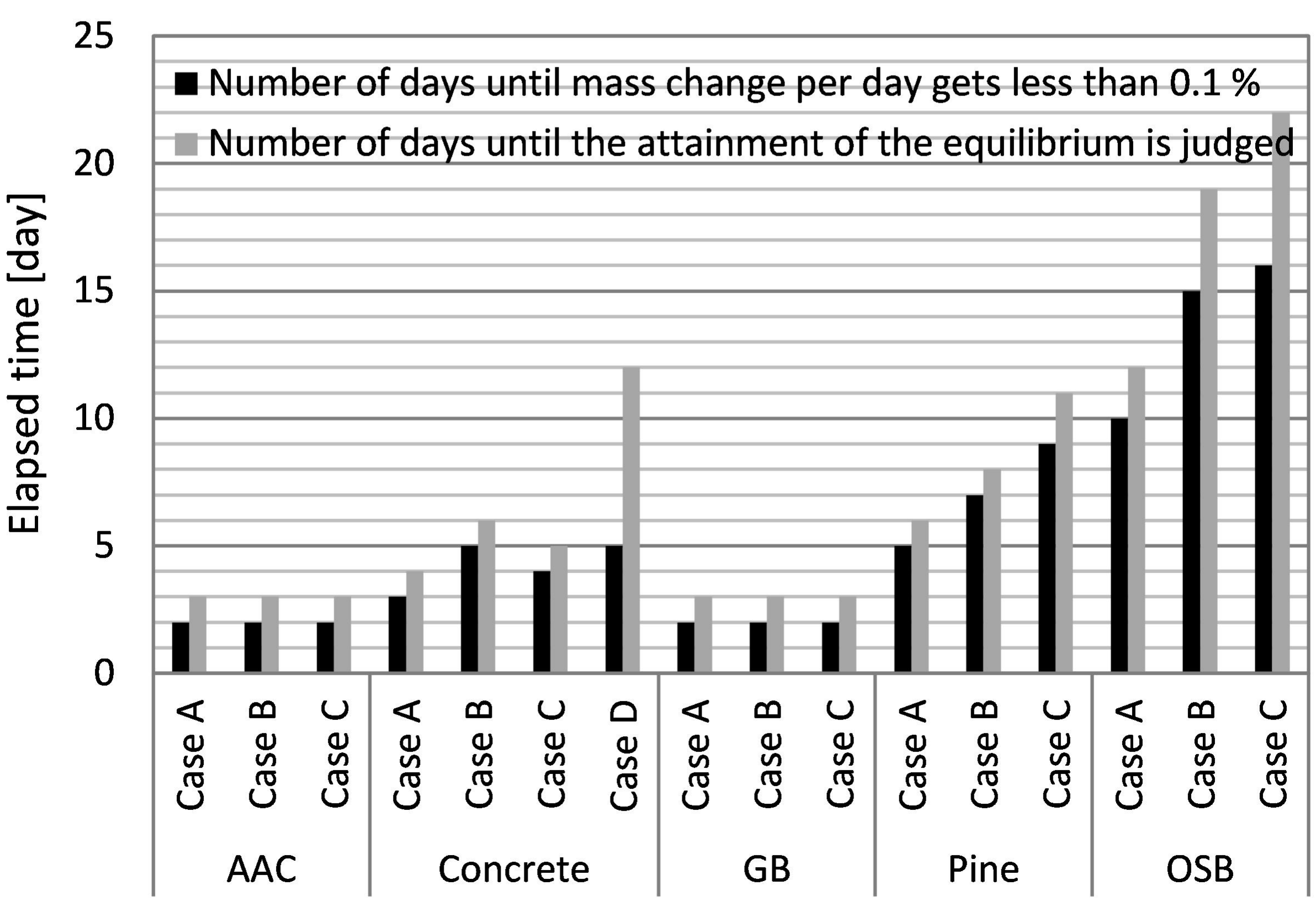
Number of days until mass change per day gets less than 0.1 %
Number of days until the attainment of the equilibrium is judged
Elapsed time [day]
0
5
10
15
20
25
Case A
Case B
Case C
Case D
AAC
Concrete
GB
Pine
OSB

(b)

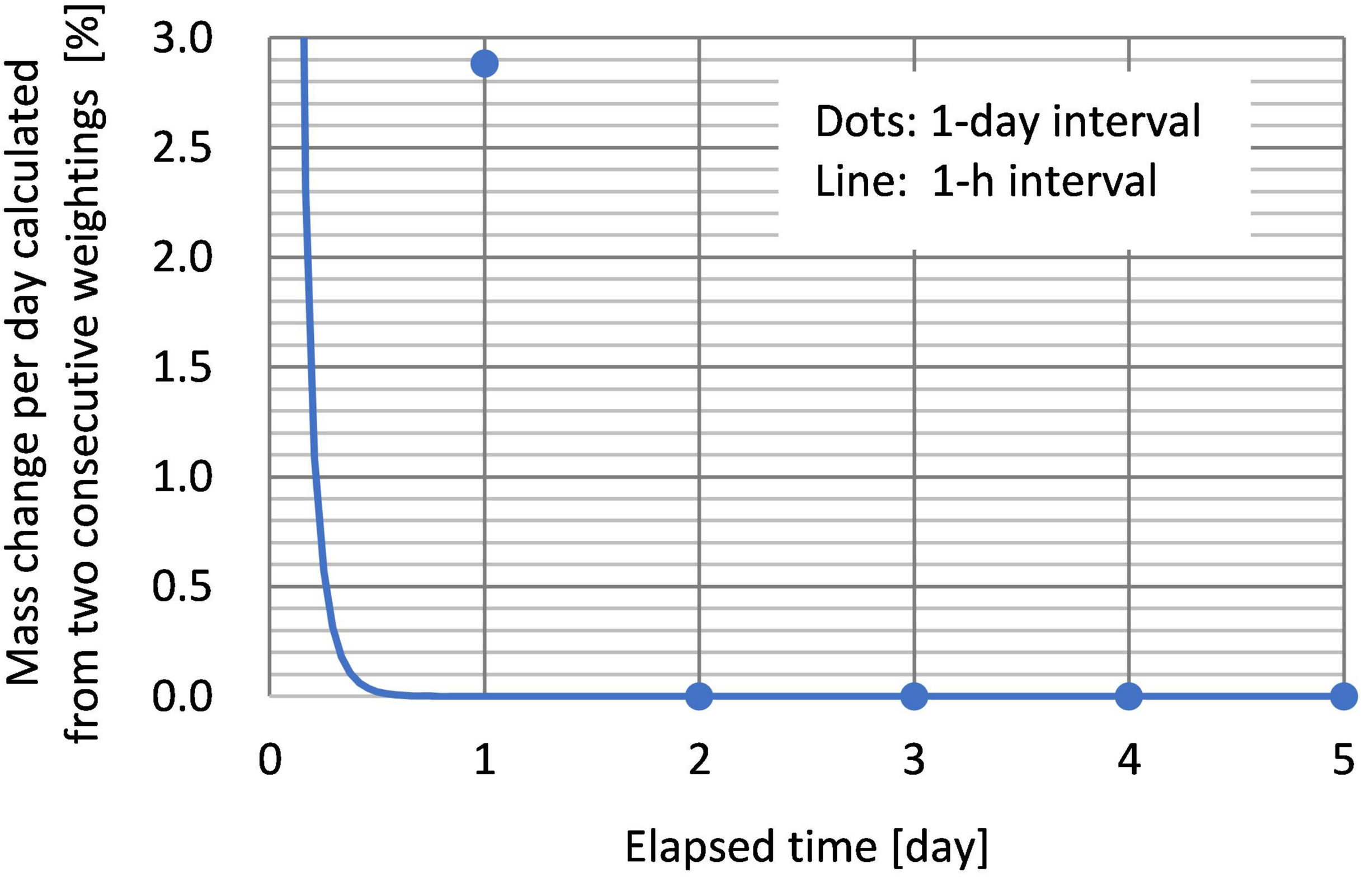
Mass change per day calculated
from two consecutive weightings [%]
3.0
2.5
2.0
1.5
1.0
0.5
0.0
Dots: 1-day interval
Line: 1-h interval
0
1
2
3
4
5
Elapsed time [day]

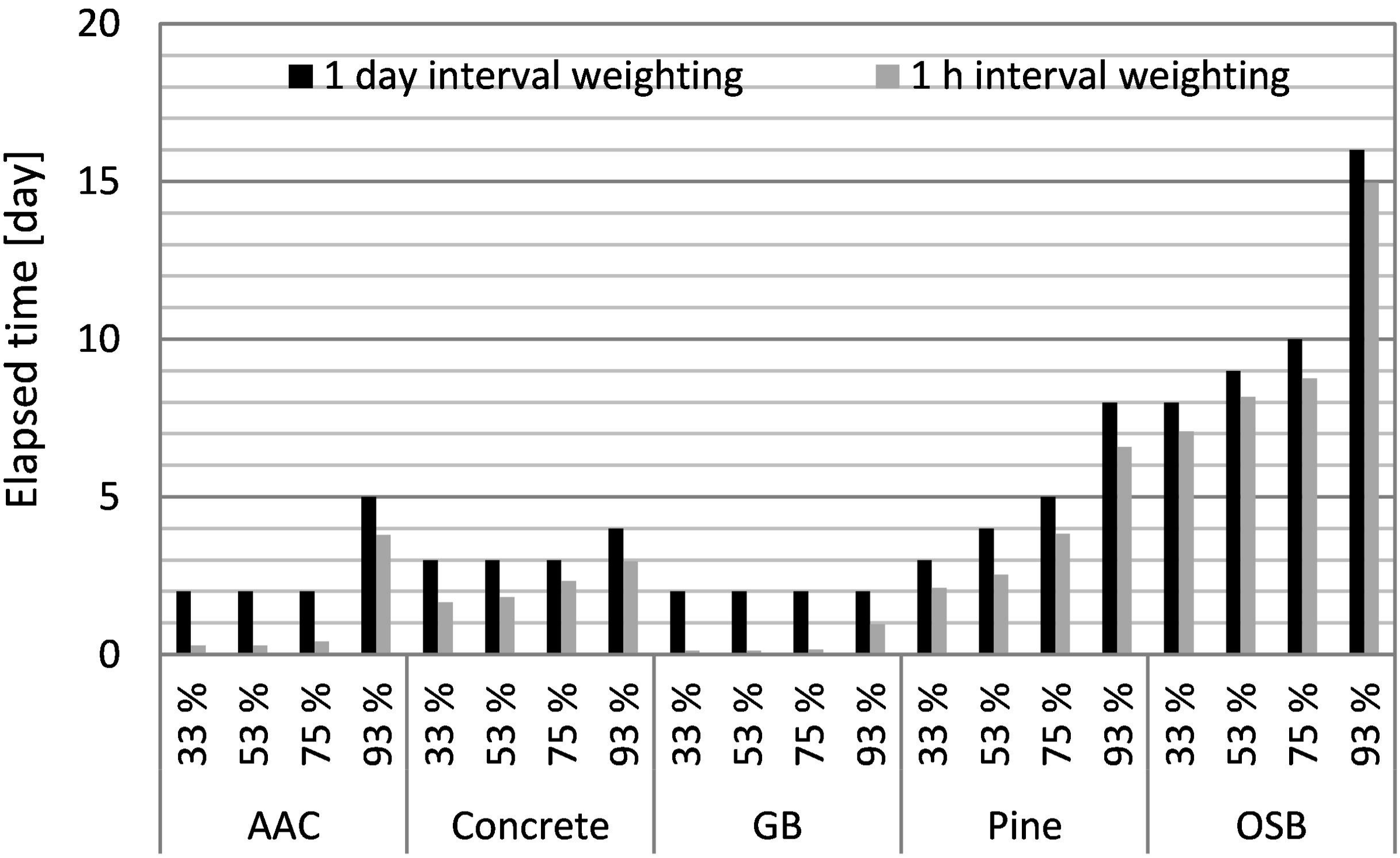
20
15
10
5
0
Elapsed time [day]
1 day interval weighting
1 h interval weighting
33 %
53 %
75 %
93 %
AAC
Concrete
GB
Pine
OSB

(a)

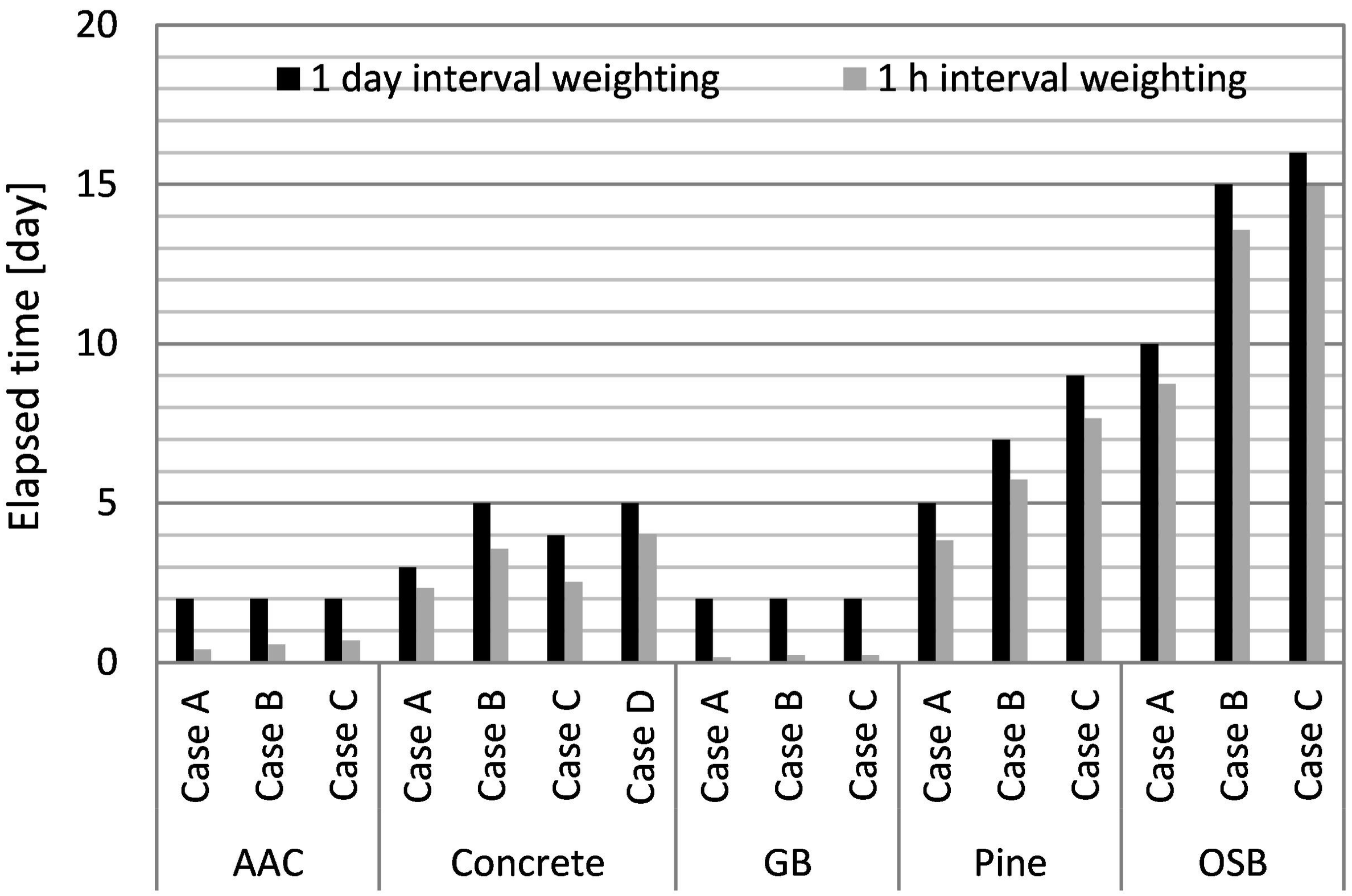
20
15
10
5
0
Elapsed time [day]
1 day interval weighting
1 h interval weighting
Case A
Case B
Case C
Case D
AAC
Concrete
GB
Pine
OSB

(b)

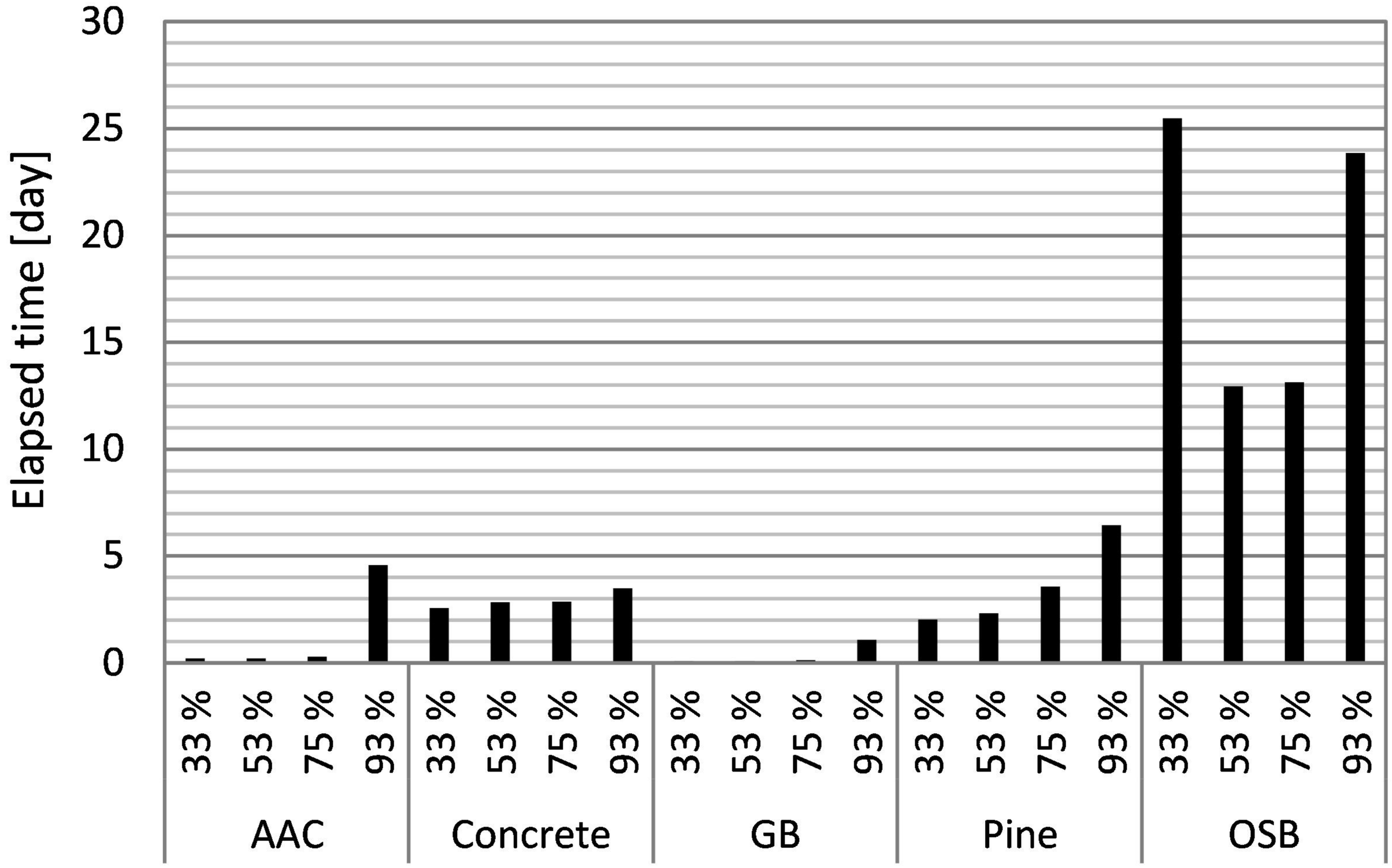
Elapsed time [day]
30
25
20
15
10
5
0
33 %
53 %
75 %
93 %
AAC
Concrete
GB
Pine
OSB

(a)

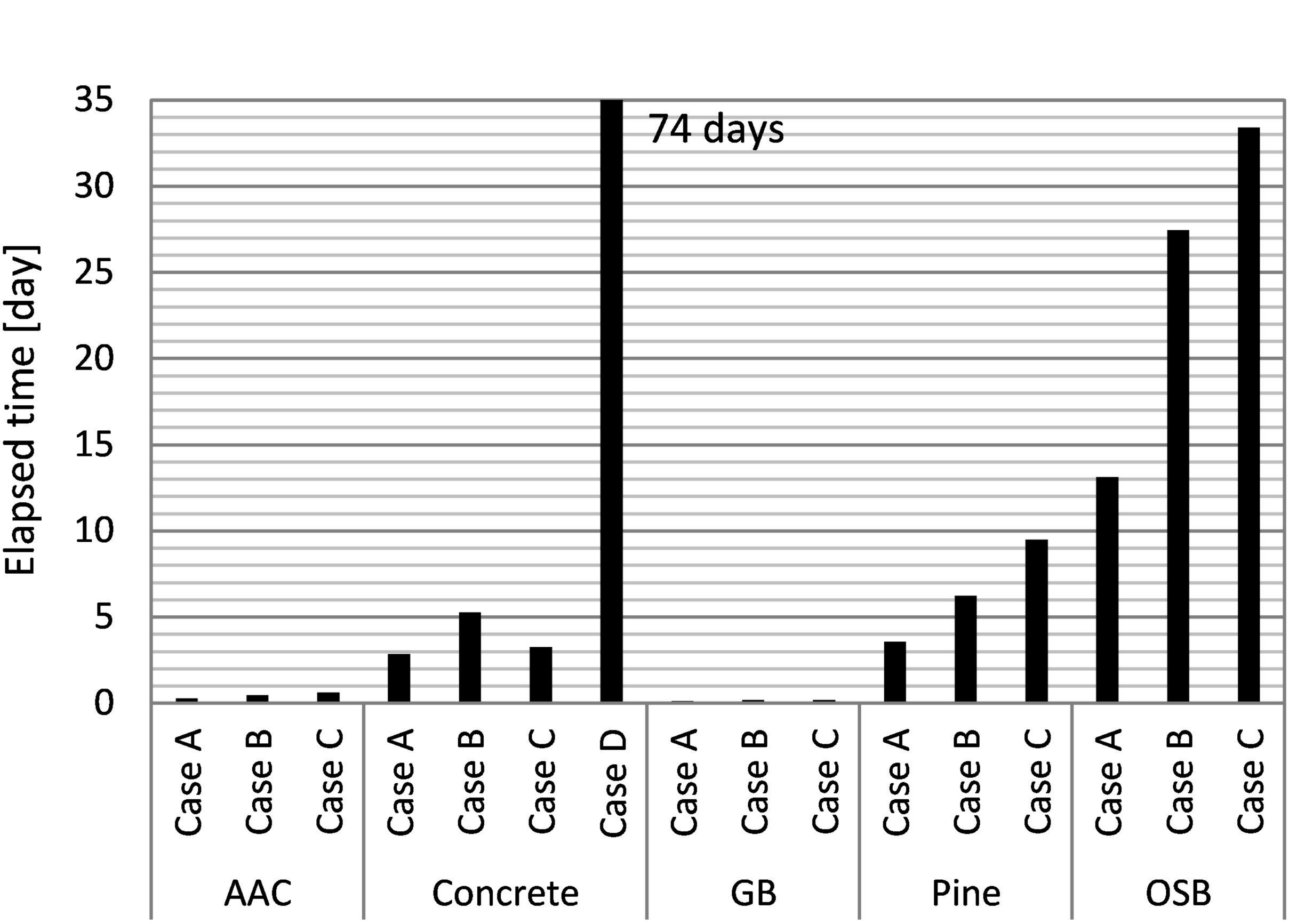
Elapsed time [day]
35
30
25
20
15
10
5
0
74 days
Case A
Case B
Case C
Case D
AAC
Concrete
GB
Pine
OSB

(b)